



ComEd
Energy Efficiency Program



Performance Assessment of High Efficiency Variable Speed Air-Source Heat Pump in Cold Climate Applications

Gregory Shoukas, Eric Bonnema, Gokulram Paranjothi,
Ramin Faramarzi, and Lauren Klun

*Produced under direction of ComEd by the National Renewable Energy Laboratory (NREL)
under Technical Services Agreement TSA-19-01159*

**NREL is a national laboratory of the U.S. Department of Energy
Office of Energy Efficiency & Renewable Energy
Operated by the Alliance for Sustainable Energy, LLC**

This report is available at no cost from the National Renewable Energy Laboratory (NREL) at www.nrel.gov/publications.

Contract No. DE-AC36-08GO28308

**Strategic Partnership Project Report
NREL/TP-5500-80802
February 2022**



ComEd
Energy Efficiency Program

Performance Assessment of High Efficiency Variable Speed Air-Source Heat Pump in Cold Climate Applications

Gregory Shoukas, Eric Bonnema, Gokulram Paranjothi,
Ramin Faramarzi, and Lauren Klun

Suggested Citation

Shoukas, Gregory, Eric Bonnema, Gokulram Paranjothi, Ramin Faramarzi, and Lauren Klun. 2022. *Performance Assessment of High Efficiency Variable Speed Air-Source Heat Pump in Cold Climate Applications*. Golden, CO: National Renewable Energy Laboratory. NREL/TP-5500-80802. <https://www.nrel.gov/docs/fy22osti/80802.pdf>.

**NREL is a national laboratory of the U.S. Department of Energy
Office of Energy Efficiency & Renewable Energy
Operated by the Alliance for Sustainable Energy, LLC**

This report is available at no cost from the National Renewable Energy Laboratory (NREL) at www.nrel.gov/publications.

Contract No. DE-AC36-08GO28308

Strategic Partnership Project Report
NREL/TP-5500-80802
February 2022

National Renewable Energy Laboratory
15013 Denver West Parkway
Golden, CO 80401
303-275-3000 • www.nrel.gov

NOTICE

This work was authored by the National Renewable Energy Laboratory, operated by Alliance for Sustainable Energy, LLC, for the U.S. Department of Energy (DOE) under Contract No. DE-AC36-08GO28308. Support for the work was also provided by ComEd through CLEAResult under TSA-19-01159. The views expressed in the article do not necessarily represent the views of the DOE or the U.S. Government.

The ComEd Energy Efficiency Program is funded in compliance with state law.

This report is available at no cost from the National Renewable Energy Laboratory (NREL) at www.nrel.gov/publications.

U.S. Department of Energy (DOE) reports produced after 1991 and a growing number of pre-1991 documents are available free via www.OSTI.gov.

Cover photo from iStock 1180689542.

NREL prints on paper that contains recycled content.

Acknowledgments

The authors would like to thank the ComEd Energy Efficiency Program and CLEARResult for supporting this research. Additionally, thanks to the National Renewable Energy Laboratory's Eric Kozubal for his experimental support and expert guidance related to high-altitude HVAC characterization, and Korbaga Woldekidan for enhancing the EnergyPlus® engine and performing energy simulations.

The authors would also like to express their sincere gratitude to Steven Labarge of ComEd and Brittany Zwicker of CLEARResult for their in-depth report review.

This report was prepared by the National Renewable Energy Laboratory (NREL), operated by Alliance for Sustainable Energy, LLC, for the U.S. Department of Energy (DOE) under Contract No. DE-AC36-08GO28308. Funding provided by CLEARResult under Technical Services Agreement No. TSA-19-01159.

For more information, contact:

Greg Shoukas
National Renewable Energy Laboratory
Email: greg.shoukas@nrel.gov

Eric Bonnema
National Renewable Energy Laboratory
Email: eric.bonnema@nrel.gov

Gokul Paranjothi
National Renewable Energy Laboratory
Email: gokulram.paranjothi@nrel.gov

List of Acronyms

| | |
|--------|---|
| AHRI | Air-Conditioning, Heating, and Refrigeration Institute |
| AHU | air-handler unit |
| ANSI | American National Standards Institute |
| ASHRAE | American Society of Heating, Refrigerating and Air-Conditioning Engineers |
| ASME | American Society of Mechanical Engineers |
| BTU | British Thermal Unit |
| ComEd | Commonwealth Edison Company |
| COP | coefficient of performance |
| db | dry-bulb |
| dp | dew-point |
| DOE | U.S. Department of Energy |
| DX | direct expansion |
| EER | energy efficiency ratio |
| HSPF | heating seasonal performance factor |
| HVAC | heating, ventilating, and air conditioning |
| NREL | National Renewable Energy Laboratory |
| OAT | outdoor air (dry-bulb) temperature |
| OU | outdoor unit |
| RA | return airstream |
| RPM | revolutions per minute |
| RSM | response surface methodology |
| SEER | seasonal energy efficiency ratio |
| SHR | sensible heat ratio |
| TC | thermocouple |
| TMY | typical meteorological year |
| TTF | Thermal Test Facility |
| wb | wet-bulb |

Executive Summary

This project was part of an effort by ComEd's emerging technology program to evaluate the energy saving potential of new energy efficiency technologies. The focus of this technology assessment was to determine energy and peak demand savings potentials of a high-efficiency variable-speed, air-source, split system heat pump designed for cold climate applications. The results of this technology assessment will be used by ComEd and CLEAResult to determine considerations for future offerings in ComEd's Energy Efficiency Program.

The project utilized the National Renewable Energy Laboratory's (NREL) Thermal Test Facility to experimentally characterize cooling and heating performance of a high-efficiency heat pump split system under varying indoor and outdoor climate conditions. The selected climate conditions represented summer and low-temperature winter conditions in ComEd's service territory. The laboratory experimentation results were used to develop equipment performance curves required by the EnergyPlus[®] hourly simulation engine. Using typical meteorological year 3 weather data for the Chicago O'Hare airport, hourly building simulations (using the EnergyPlus engine) was utilized to estimate the annual energy savings of the high-efficiency heat pump in comparison to a standard efficiency heat pump unit in the following U.S. Department of Energy's (DOE) building codes program energy prototypes:

1. Single-family home
2. Strip mall
3. Low-rise office.

Figure ES-1 depicts the annual whole-building cooling and heating energy savings per square foot of conditioned floor area:

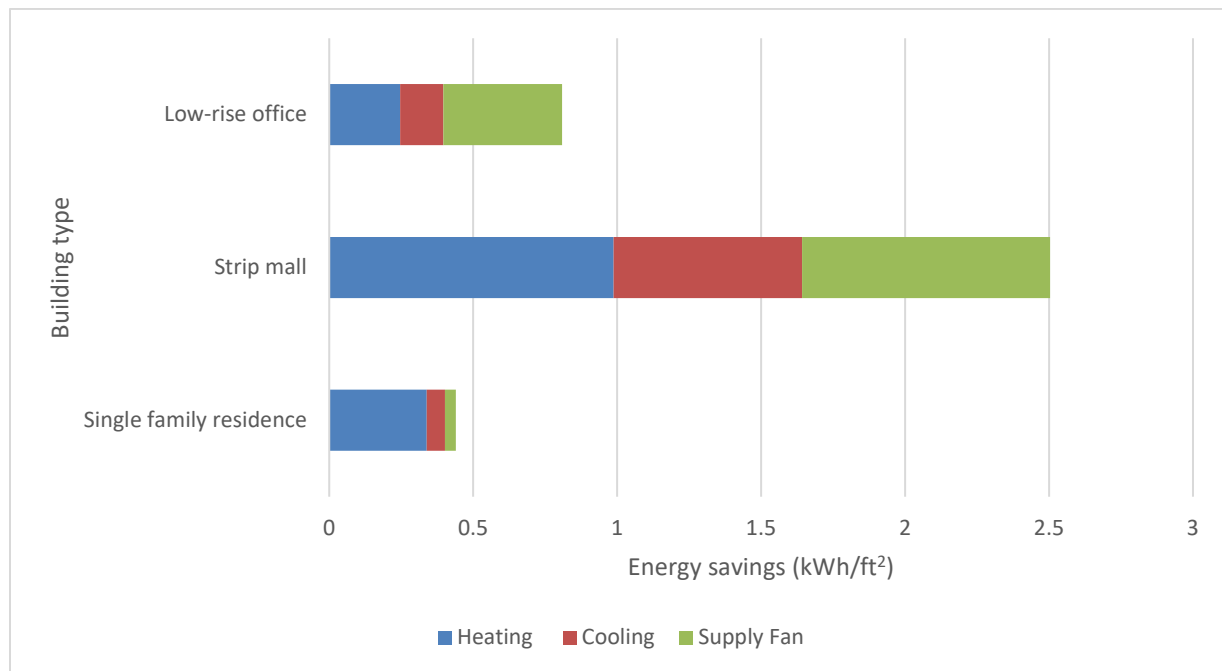


Figure ES-1. Energy savings per floor area for each building type and end use

Table of Contents

| | | |
|--------------------|---|-----------|
| 1 | Introduction | 1 |
| 1.1 | Technology Description | 2 |
| 1.2 | Project Goals | 3 |
| 2 | Experimental Configuration | 3 |
| 2.1 | Laboratory Setup | 4 |
| 2.2 | Measurement and Instrumentation Plan | 10 |
| 3 | Experimentation Plan | 12 |
| 3.1 | Embedded Controls and Limits of Operation..... | 13 |
| 3.2 | Design of Experiment..... | 18 |
| 3.3 | Testing Adjustments and Measured Performance Corrections | 21 |
| 3.4 | Characterizing the Equipment Performance..... | 24 |
| 3.5 | Regressing the Performance Data | 29 |
| 4 | Energy Modeling Setup | 34 |
| 5 | Energy Modeling Results | 35 |
| 6 | Conclusion | 38 |
| Appendix A. | Instrumentation Plan | 40 |
| Appendix B. | Test Matrix | 42 |
| Appendix C. | Steady-State Cooling Performance | 45 |
| Appendix D. | Steady-State Heating Performance | 47 |
| Appendix E. | Accuracy of RSM Predictive Cooling Model Regressions | 49 |
| Appendix F. | Accuracy of RSM Predictive Heating Model Regressions | 51 |
| Appendix G. | Heating Defrost Cycle | 53 |

List of Figures

| | |
|--|----|
| Figure ES-1. Energy savings per floor area for each building type and end use | v |
| Figure 1. TTF laboratory containing four inlet and outlet airstreams..... | 3 |
| Figure 2. Internal view of the Carrier Infinity Series (FE4A) indoor unit (air-handler)..... | 5 |
| Figure 3. Air-handler (indoor unit), test article mounted on inlet (bottom) and outlet (top) plenums..... | 6 |
| Figure 4. Outdoor unit, test article | 7 |
| Figure 5. Environmental test chamber used to create an outdoor climate around the test article..... | 8 |
| Figure 6. Outdoor unit set inside environmental chamber (left); environmental chamber connected to the TTF airstreams (right)..... | 9 |
| Figure 7. Variable speed limits when the compressor operates in cooling mode | 14 |
| Figure 8. Variable speed limits when the compressor operates in heating mode | 15 |
| Figure 9. Air-handler unit flow rates for two modes of cooling operation; data points represent the performance lookup table generated across a broad range of indoor and outdoor conditions..... | 16 |
| Figure 10. Air-handler unit supply air temperature for the two modes of heating operation; data points represent the performance lookup table generated across a broad range of indoor and outdoor conditions | 17 |
| Figure 11. Supply air temperatures with respect to the outdoor air temperature and mode of operation based on the performance lookup table..... | 17 |
| Figure 12. Electrical power consumption of the outdoor fan unit relative to fan speed | 22 |
| Figure 13. Controlling the compressor speed by emulating a room temperature signal on the thermostat | 25 |
| Figure 14. Thermostat and instrumentation on the indoor unit..... | 26 |
| Figure 15. Compressor speed during the defrost cycle as a function of the outdoor air temperature..... | 28 |
| Figure 16. Defrost and performance degradation cycles over an 8-hour period maintaining an outdoor air temperature of 28°F..... | 29 |
| Figure 17. Expected range of varying heating capacity and COP versus outdoor air temperatures | 31 |
| Figure 18. Estimated capacity derating factors regressions to account for defrost cycles..... | 33 |
| Figure 19. COP derating as a function of the capacity derating factor | 33 |
| Figure 20. HVAC energy use comparison for a single-family home with the high-efficiency heat pump model. The figure on the left shows the end-use savings breakdown, and the figure on the right shows the total site energy use for the baseline and high-efficiency heat pump models. | 36 |
| Figure 21. HVAC energy use comparison for a strip mall with the high-efficiency heat pump model. The figure on the left shows the end-use energy consumption breakdown, and the figure on the right shows the total site energy use for the baseline and high-efficiency heat pump models. | 36 |
| Figure 22. HVAC energy use comparison for low-rise office building with the high-efficiency heat pump model. The figure on the left shows the annual end-use energy consumption breakdown, and the figure on the right shows the total site annual energy use for baseline and the high-efficiency heat pump model. | 37 |
| Figure 23. JMP statistical software RSM predictive model accuracy (U95) of the heat pump cooling regressions in comfort mode | 49 |
| Figure 24. JMP statistical software RSM predictive model accuracy (U95) of the heat pump cooling regressions in efficiency mode..... | 50 |
| Figure 25. JMP statistical software RSM predictive model accuracy (U95) of the heat pump heating regressions in comfort mode | 51 |
| Figure 26. JMP statistical software RSM predictive model accuracy (U95) of the heat pump heating regressions in efficiency mode..... | 52 |
| Figure 27. Defrost embedded control logic explained in the Carrier 25VNA0 service manual | 53 |

List of Tables

| | |
|--|----|
| Table 1. Table of Manufacturer’s Performance Specifications | 2 |
| Table 2. Power Measurement Sensors | 10 |
| Table 3. Air Flow Rate Measurement Sensors | 11 |
| Table 4. Heating/Cooling Capacity Measurement Sensors..... | 11 |
| Table 5. Heating/Cooling Capacity Measurement Sensors..... | 11 |
| Table 6. Additional Measurements and Sensors | 12 |
| Table 7. Factors and Ranges Specified to Develop the Cooling Design of Experiment Test Matrix | 19 |
| Table 8. Factors and Ranges Specified to Develop the Steady-State Heating Design of Experiment Test Matrix..... | 20 |
| Table 9. Independent Variables, Measured and Calculated Performance Values Used in the RSM Cooling Predictive Models | 30 |
| Table 10. Independent Variables, Measured and Calculated Performance Values Used in the RSM Heating Predictive Models..... | 31 |
| Table 11. Summary of Different DOE Prototype Buildings Simulated..... | 34 |
| Table 12. Energy Savings Summary for the Different DOE Prototype Buildings Simulated | 38 |
| Table 13. Critical Experimental Measurements and Sensors..... | 40 |
| Table 14. Cooling (Wet-Coil) Steady-State Test Conditions (Comfort Mode and Efficiency Mode) | 42 |
| Table 15. Cooling (Dry-Coil) Steady-State Test Conditions (Comfort Mode and Efficiency Mode)..... | 43 |
| Table 16. Heating Steady-State Test Conditions (Comfort Mode and Efficiency Mode) | 44 |
| Table 17. Test Conditions and Heat Pump Cooling Performance Adjusted for Sea Level Operation in Efficiency Mode..... | 45 |
| Table 18. Test Conditions and Heat Pump Cooling Performance Adjusted for Sea Level Operation in Comfort Mode..... | 46 |
| Table 19. Test Conditions and Heat Pump Heating Performance Adjusted for Sea Level Operation in Efficiency Mode..... | 47 |
| Table 20. Test Conditions and Heat Pump Heating Performance Adjusted for Sea Level Operation in Comfort Mode..... | 48 |

1 Introduction

This project was part of an effort by ComEd's emerging technology program to evaluate the energy saving potential of new energy efficiency technologies. The focus of this technology assessment was to determine energy and peak demand savings potentials of a high-efficiency variable-speed, air-source, split system heat pump designed for cold climate applications. The results of this technology assessment will be used by ComEd and CLEAResult to determine considerations for future offerings in ComEd's Energy Efficiency Program.

Recent advances in heat pump systems employ variable-speed compressor technology and electronically commutated fan motors. Compared to single-speed heat pumps, variable-speed systems can maintain higher heating and cooling efficiencies over a wider range of outdoor temperatures. For any given heat pump speed, the thermal capacity inherently decreases with falling outdoor temperatures. Variable-speed heat pumps can ramp up the compressor to increase the thermal output and compensate for the reduced capacity at lower outdoor temperatures. These advances are commercially available in a few configurations such as minisplit, multisplit, and ducted split systems. These system configurations are predominately used in residential applications.

This project utilized the HVAC Laboratory located at the National Renewable Energy Laboratory's (NREL) Thermal Test Facility (TTF) to experimentally characterize cooling and heating performance of a high-efficiency split system heat pump under varying outdoor climate conditions. The selected climate conditions represented summer and low-temperature winter conditions in ComEd's service territory. The laboratory experimentation results were used to develop equipment performance tables that could be used by the EnergyPlus[®] building simulation engine. Using typical meteorological year 3 (TMY3) weather data for the Chicago O'Hare airport, hourly building simulations (using the EnergyPlus engine) was utilized to estimate the annual energy savings of the high-efficiency heat pump in comparison to a standard efficiency unit in the following U.S. Department of Energy's (DOE) building codes program energy prototypes:

1. Single-family home
2. Strip mall
3. Low-rise office.

This document reports on the approach and results of the laboratory experimentation work and the building simulations associated with a high-efficiency, variable-speed heat pump designed for operation in cold climates. The document is organized as follows:

- Section 1 summarizes the technology description and project goals
- Section 2 details the experimental configuration and laboratory setup
- Section 3 documents the testing approach for performance mapping the equipment
- Section 4 discusses the EnergyPlus modeling approach
- Section 5 summarizes the annual energy savings results.

1.1 Technology Description

The test unit used for this study was a five-ton Carrier® Infinity® Series heat pump with Greenspeed® (variable speed) intelligence. Table 1 summarizes the specifications of this unit.

Table 1. Table of Manufacturer’s Performance Specifications

| Carrier Infinity Series with Greenspeed Intelligence | | |
|---|-------------------------|----------------------------|
| Outdoor Unit (25VNA0060A) / Air-Handler Unit (FE4ANB006) / Thermostat (SYSTXCCITC01-B) | | |
| | Cooling | Heating |
| Rated Capacity ^{1,2} [BTU/h] | 56,000 | 55,500 |
| SEER ¹ [-] | 18.0 | - |
| EER ¹ [-] | 12.7 | - |
| Compressor Speed [RPM] | 1,800–4,250 | 1,800–7,000 |
| Outdoor Unit Fan Speed [RPM] | 500–900 | 500–900 |
| Indoor Unit Fan Speed [RPM] | 1,185–1,885 | 750–1,750 |
| Expansion Device | Thermal expansion valve | Electronic expansion valve |
| HSPF ² [-] | - | 12.0 |
| COP ² [-] @ 47°F | - | 3.86 |
| COP ³ [-] @ 17°F | - | 2.22 |

¹ Cooling standard: 80°F (27°C) db 67°F (19°C) wb indoor entering air temperature and 95°F (35°C) db air entering outdoor unit.

² High heating standard: 70°F (21°C) db indoor entering air temperature and 47°F (8°C) db 43°F (6°C) wb air entering outdoor unit.

³ Low heating standard: 70°F (21°C) db indoor entering air temperature and 17°F (-8°C) db 15°F (-9°C) wb air entering outdoor unit.

The Carrier heat pump’s steady-state heating and cooling performance was evaluated over a wide range of outdoor conditions and typical indoor conditions. The thermal capacity and coefficient of performance (COP), a unitless measure of heating or cooling capacity over total power input, was assessed over the range of conditions discussed in Section 3.

In addition, two modes of equipment operation were characterized: comfort and efficiency mode. Comfort mode operates the equipment to provide better dehumidification during cooling and higher supply air temperatures during heating. Efficiency mode operates the equipment to provide the best energy efficiency while satisfying the thermostat temperature setpoint.

NREL designed an experimentation plan such that the unit operates under its embedded control algorithms to ensure a realistic assessment of the operation, performance, and energy consumption while varying environmental conditions. This operating approach is the most representative of the equipment’s actual operation in a building and differs from the rating methodology outlined in the AHRI 210/240 (AHRI 2023) standard. This standard requires performance evaluation of the heat pump under limited test conditions while overriding the embedded controls via a third mode of operation called technician checkout mode.

1.2 Project Goals

The goal of this project is to estimate the energy and demand savings of the high-efficiency heat pump in selected building types under typical Chicago-area weather. Steady-state heating and cooling performance data from laboratory experimentations were used to develop equipment performance tables. Performance tables were then integrated to the EnergyPlus (DOE 2021) simulation platform for modeling the energy performance of the high-efficiency heat pump in the following building types using typical Chicago-area weather data:

1. Single-family home
2. Strip mall
3. Low-rise office.

2 Experimental Configuration

The TTF is a 100% outdoor air psychrometric laboratory that delivers conditioned air to a test article. Through a custom, computer-based measurement and data acquisition system, the lab controls and maintains precise air temperature, humidity, pressures, and flow rates to precise setpoints. Four laboratory air streams in total are used to control and measure the psychrometric conditions at the inlet and outlet of the indoor and outdoor unit. Accurate, real-time measurements are recorded to determine the heat and mass transfer performance of HVAC equipment. Figure 1 highlights TTF's layout of the four inlet and exhaust airstreams used to test HVAC systems up to 10 tons in capacity.

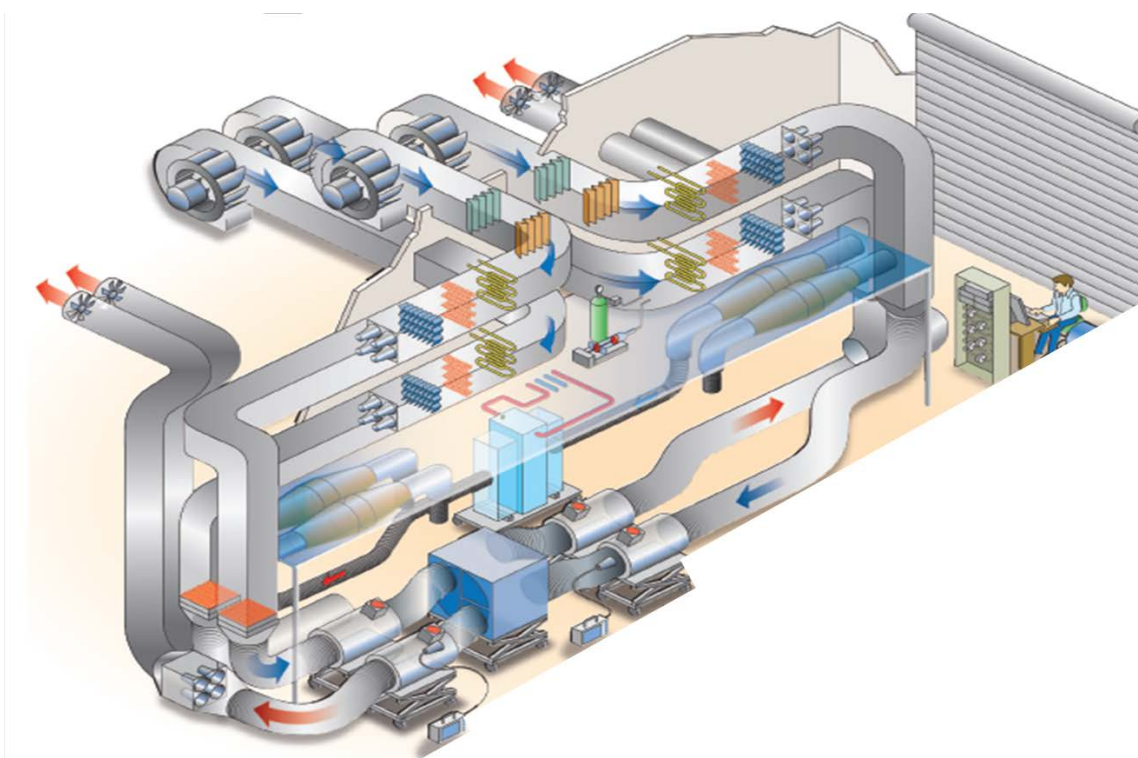


Figure 1. TTF laboratory containing four inlet and outlet airstreams

Figure by NREL

Generally, testing methods and laboratory measurements are guided by ASME, ANSI, AHSRAE and AHRI standards. Although this project foundationally followed these standards, it did not strictly conform to them. For example, standards ANSI/ASHRAE 37 (ASHRAE 2019) and AHRI 210/240 (AHRI 2023) provide a framework for testing that result in a single rating value such as seasonal energy efficiency ratio (SEER) or heating seasonal performance factor (HSPF). Although these single point ratings provide a good comparative metric for consumers, they are insufficient for characterizing the equipment performance over a range of operational conditions, which is needed in building energy simulation.

2.1 Laboratory Setup

Providing precise and constant temperature and humidity conditions to the indoor and outdoor unit is essential for steady-state performance evaluations. Prior to collecting performance data, NREL test engineers ensured steady-state operation was achieved by monitoring in real-time the psychrometric conditions supplied to the indoor and outdoor.

Custom plenums were built around the indoor unit (air-handler) and connected to the laboratory's air streams. The TTF can generate and supply directly a wide range of psychrometric conditions to characterize the indoor unit. The laboratory fans assist the air-handler and provide conditioned air, at the proper volumetric flow rates and external static pressures during experimentation.

The lab can also generate a wide range of hot and humid psychrometric test conditions to characterize the outdoor unit in cooling mode. However, the existing TTF setup cannot directly supply the outdoor test article the extremely cold air conditions needed to replicate Chicago winters. Consequently, the NREL team had to design and build a custom environmental chamber to allow heating cycle evaluations that mimic Chicago's low ambient winter conditions. The heat pump outdoor unit, situated inside the environment chamber, would assist cooling the chamber to extremely cold conditions. The cold air leaving the outdoor unit would be recirculated until the desired cold test conditions were reached. Once the cold temperature was achieved, the TTF would trim the setpoints by adding heat or humidity to maintain steady-state conditions throughout the experiment.

The experimental design and setup for the indoor and outdoor will be discussed in the following subsections.

2.1.1 Indoor Unit

The test article's indoor unit comprises a refrigerant coil that provides heating or cooling, a thermal expansion valve, a variable-speed electronically commutated blower motor, and a control board as seen in Figure 2. In the pictured configuration, the blower draws air from the bottom of the cabinet through the refrigerant coil. The conditioned air then passes through the blower where it exits the top of the cabinet and provides supply air to the building. This cabinet allows for the condensate drain pan to be moved so the air-handling unit can be oriented horizontally or vertically.



Figure 2. Internal view of the Carrier Infinity Series (FE4A) indoor unit (air-handler)

All photos by Greg Shoukas, NREL

The air-handler is mounted on top of insulated plenums such that the air, guided by turning vanes, makes a 90° turn at the cabinet's inlet and outlet. This method has been validated from prior research projects (Wheeler and Pate 2016). The TTF supplies and exhausts air across the indoor unit through 18-inch flexible ducts that are connected and clamped to the round collars. The indoor unit test setup can be seen in Figure 3.



Figure 3. Air-handler (indoor unit), test article mounted on inlet (bottom) and outlet (top) plenums

A set of four static pressure taps are installed in each of the plenums to measure the external static pressure across the unit using a differential pressure transducer. Air blenders are installed in the inlet and outlet plenums to blend the air for a homogenous temperature measurement using an averaging array of thermocouples (TC) (ANSI/ASHRAE, 41.1-2013). An air sampling rake draws from each of the air streams to measure dew-point using chilled mirror hygrometers (ANSI/ASHRAE, 41.6-2014). Inlet and outlet air mass flow rates are measured using ASME flow nozzles, a thermocouple, and two differential pressure transducers with a combined uncertainty of less than 2% compliant with ANSI/ASHRAE, 41.2-2018. The indoor unit blower speed is measured using an optical tachometer mounted inside the air-handler and positioned to view the rotating fan cage. The indoor unit control board is connected to the outdoor unit control

board and a Carrier Infinity Touch communicating thermostat. The thermostat communicates with both units to provide cooling or heating at the proper speeds. Further explanations of the thermostat are discussed in Section 3.

2.1.2 Outdoor Unit

The Carrier outdoor unit is composed of four main components: a variable-speed electrically commutated fan, an outdoor refrigerant coil, a variable-speed scroll compressor, and a variable frequency drive (inverter). This is shown in Figure 4.



Figure 4. Outdoor unit, test article

Image from Carrier (Carrier Corporation, 2018)

During operation, the outdoor unit's variable-speed fan draws air through the coil from four sides and exhausts it from the top of the unit. The fan speed is determined based on the outdoor air temperature. The variable-speed compressor moves refrigerant in a closed loop through the coils of the indoor and the outdoor units. Depending on whether the system is in heating or cooling mode, the coils either extract or reject heat between the refrigerant and air. The inverter modulates the speed of the compressor to match the equipment capacity with space-conditioning load. As a result, the unit runs nearly continuously while using the minimum amount of power to meet the setpoints. This strategy allows variable-speed heat pumps to provide consistent comfort and energy savings over traditional single-speed HVAC systems, which cycle their operation causing higher fluctuations in indoor air temperature. The system's inverter controls the compressor to higher speeds during the heating mode (compared to cooling mode) to compensate

for loss of heating capacity without having to oversize the cooling capacity. Especially in cold climate zones, this is a major advantage over single-speed heat pumps because the heating requirements determine system size.

An insulated, custom environmental chamber was designed and built to conduct experimentation of the heat pump under a wide range of outdoor air conditions (Figure 5). Psychrometric conditions supplied to the inlet of the test article are controlled by mixing makeup air provided by the TTF and recirculation air from the exhaust of the outdoor test unit. The mixing takes place in the return plenum of the environmental chamber.

The proper makeup air flow rate, required to achieve the desired psychrometric (temperature and humidity) conditions at the outdoor unit inlet, is managed through a set of two dampers labeled in Figure 6. One damper allows a fraction of makeup air into the return plenum, while the second damper bypasses the excess makeup air to the TTF exhaust air stream. A booster fan draws air from the exhaust plenum and mixes it with the makeup air before returning it to the heat pump.

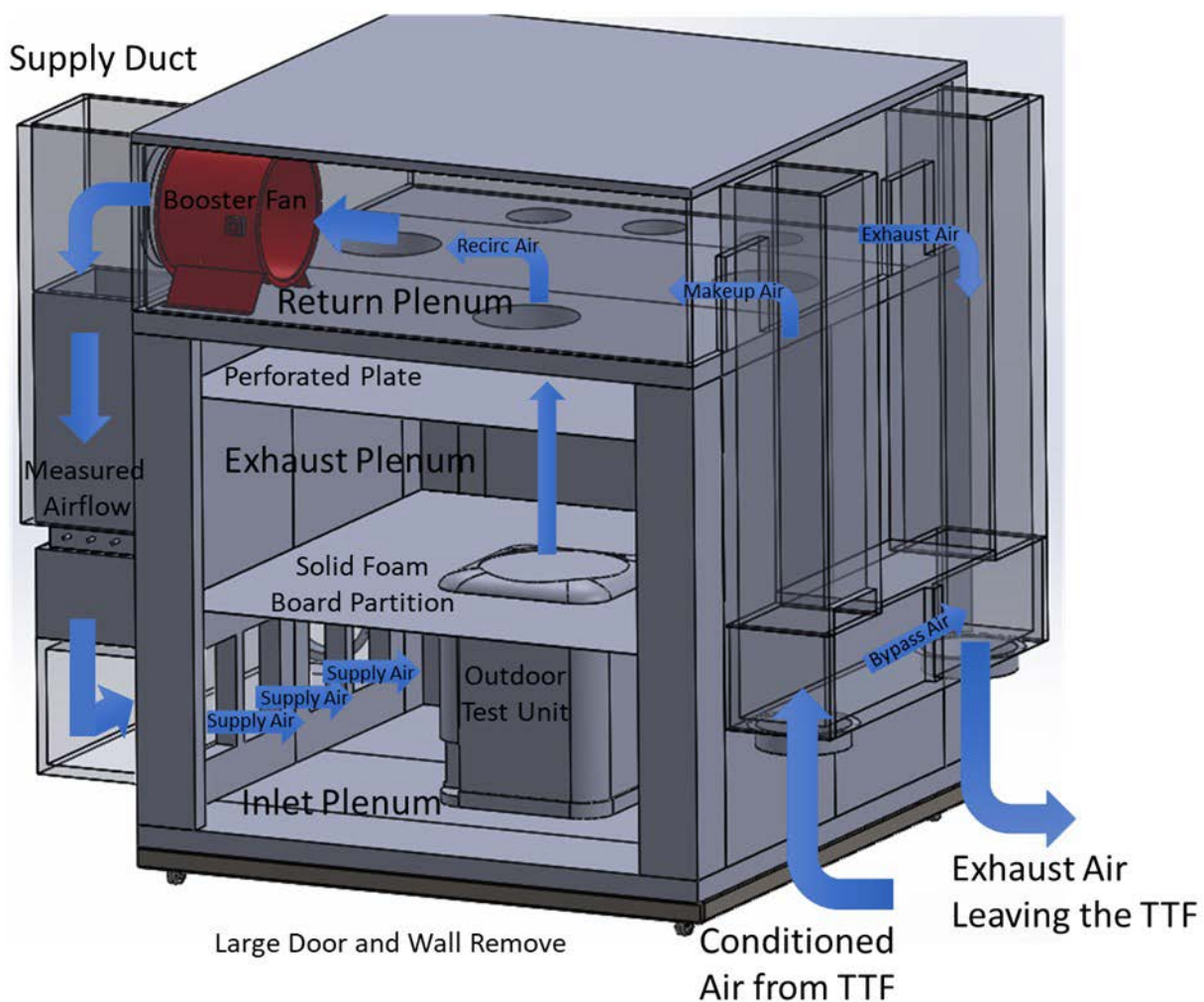


Figure 5. Environmental test chamber used to create an outdoor climate around the test article

All remaining report figures by NREL

In heating mode, recirculating the cold exhaust air from the outdoor unit lowers the temperature inside the chamber and allows it to be cooled to subzero temperatures. In cooling mode, recirculating the hot exhaust air from the outdoor unit raises the temperature inside of the chamber. To maintain a constant temperature in the chamber during heat pump experimentation, the lab exhausts a portion of the recirculated air and provide counteracting warm or cool makeup air. Similarly, humidity levels are controlled at the heat pump inlet by adjusting the humidity ratios in the makeup airstream. This control strategy maintains constant psychrometric inlet conditions during heat pump characterization for both heating and cooling modes. This technique also allows operation at temperatures below that required by AHRI standard 210/240.



Figure 6. Outdoor unit set inside environmental chamber (left); environmental chamber connected to the TTF airstreams (right)

Temperature, humidity, static pressure, and air flow measurements are taken at various points in the environmental chamber. Characterizing the inlet and exhaust, temperature, and dew-point conditions provides information related to the enthalpy exchange from the outdoor unit. Furthermore, these measurements provide the laboratory feedback information needed to adjust and condition the makeup air. The volumetric air flow rate supplied to inlet plenum via the booster fan is measured through an averaging pitot tube array.¹ Prior to testing, the pitot tube array measurements were calibrated using the TTF flow nozzles readings to ensure the precision in the recirculation air flow values. The static pressures measured in the inlet and outlet plenum allow the laboratory to control the fan speed and air flow rates to the desired experimental conditions.

¹ <https://www.dwyer-inst.com/Product/AirQuality/FlowSensors/SeriesFLST#literature>

2.2 Measurement and Instrumentation Plan

Overall, the measurement and instrumentation plan served the following two main purposes:

1. Collect data required to quantify the heat pump's capacity, power consumption, and performance
2. Provide feedback information related to the response of the laboratory, environmental chamber, or the test article.

Feedback measurements are needed to make dynamic controls adjustments to achieve stable, steady-state test conditions. The essential measurements will be discussed individually in the following sections. A complete instrumentation list including the critical measurements and sensors configured in the data acquisition and controls system can be found in Appendix A, Table 13.

2.2.1 Power

Electrical power is measured with industrial, revenue-grade power meters. A power meter requires two measurements, voltage and current. A total of three power meters were used during the heat pump laboratory experiments to monitor the power consumption of the indoor unit, the outdoor unit, and the outdoor unit fan. The difference between the total outdoor unit power and the fan power yields the power input to the inverter, which drives and modulates the compressor speed. Table 2 provides information about the power measurements.

Table 2. Power Measurement Sensors

| Model Number | Distributor | Measurement Description |
|--------------|----------------------|-------------------------|
| Acuvim II-D | Accuenergy Inc. | Voltage, energy, power |
| Accu-CT | Continental Controls | Current transducer |

2.2.2 Air Flow Rate

Volumetric air flow in the TTF airstreams is measured using in-duct nozzles and two differential pressure measurements. NREL uses American Society of Mechanical Engineers (ASME) low-beta flow nozzle arrays. In addition, temperature, dew-point, and barometric pressure measurements are required to determine the air properties such that volumetric air flow can be converted to mass flow rate.

The combined uncertainty of the nozzle box and the associated instruments results in $\pm 2\%$ accuracy in mass flow rate measurements (ANSI/ASHRAE Standard 41.2-2018). Nozzle boxes measure the mass flow rate at the inlet and outlet air stream connected to the indoor unit and the makeup and exhaust air stream of the environmental chamber.

In addition, a custom sized, averaging pitot tube array (air measurement station) is designed in the supply/recirculating ductwork of the environmental chamber. The air measurement station and differential pressure transducers are calibrated using the lab flow nozzles. Table 3 provides information about the air flow measurement sensors.

Table 3. Air Flow Rate Measurement Sensors

| Model Number | Distributor | Measurement Description |
|------------------------|-----------------------|---|
| TTF Laboratory Nozzles | NA | Air mass flow rate |
| FLST-R-18x20 | Dwyer Instruments Inc | Air flow (velocity) measurement station |
| 607-01 | Dwyer Instruments Inc | Differential (air) pressure transducer |
| 607-21 | Dwyer Instruments Inc | Differential (air) pressure transducer |

2.2.3 Capacity

ASHRAE 37 (ASHRAE 2019) specifies a primary and secondary set of mass-energy measurements for determining the cooling and heating capacity of the test article. Both sets of measurements are required to be at or less than 6% of agreement. The primary cooling/heating capacity measurements are based on air-enthalpy method and are taken across the indoor unit. The measured inlet and outlet air temperature, humidity, and air mass flow rate are used to determine the enthalpy change of the air across the cooling/heating coil. Table 4 provides information about sensors used for air-enthalpy measurements. Air-enthalpy method can also be taken across the outdoor unit, although these values have higher uncertainty due to:

- Lower accuracy of the air measurement station
- Extremely low dew-points that exceed the limit of the hygrometers, particularly when the chamber is operated at subfreezing conditions.

Table 4. Heating/Cooling Capacity Measurement Sensors

| Model Number | Distributor | Measurement Description |
|------------------------|-----------------------|-------------------------|
| TTF Laboratory Nozzles | NA | Air mass flow rate |
| Type-T, TC Wire Array | Omega Engineering Inc | Air temperature |
| SIM-12H | General Eastern | Dew-point hygrometer |

Secondary cooling/heating capacity measurements are made based on refrigerant enthalpy method. This methodology relies on mass energy balance of refrigerant across cooling/heating coil. In addition to refrigerant mass flow rate, refrigerant temperature and pressures measurements will be used to quantify the thermodynamic properties of the refrigerant. The refrigerant flow meter measurements only provide accurate results when the refrigerant is in a pure liquid phase and therefore cannot always be relied upon. A sight-glass was placed in the refrigerant line to provide a visual indication of the state of refrigerant. Table 5 provides information about the sensors that were used to establish refrigerant mass energy balance.

Table 5. Heating/Cooling Capacity Measurement Sensors

| Model Number | Distributor | Measurement Description |
|-------------------------|-----------------------|-------------------------|
| Elite Series CMF025 | Micro Motion | Mass flow rate |
| Type-T, Adhesive Pad TC | Omega Engineering Inc | Surface temperature |
| PX309-1KG5V | Omega Engineering Inc | Pressure |
| Baratron 220D | MKS Instruments | Barometric pressure |

2.2.4 Feedback Measurements and Test Loop Instrumentation

In addition to power, air flow rate, temperature, and relative humidity measurements, various additional sensors are required to perform these experiments. These measurements are important to determine the test article response and provide feedback controls for stable laboratory operation. Furthermore, these measurements are used to make calculated corrections to the performance data in postprocessing. Due to testing at altitude in Golden, Colorado (5,865 ft above sea level), the measured performance data represents the equipment operation in a lower, air density (“thin-air”) environment whereby standard air pressure is 0.817 bar. Postprocessing data for thermodynamic and power corrections are required to adjust the high-altitude performance to the expected heat pump performance as if operating at sea level conditions. Table 6 lists information about the additional sensors that were used. A description of the methodology is described by Wheeler et al. (2018).

Table 6. Additional Measurements and Sensors

| Model Number | Distributor | Measurement Description |
|------------------|-----------------------|---|
| 239 | Setra Systems Inc | Differential (air) pressure transducer |
| Type-T, TC Probe | Omega Engineering Inc | Dry-bulb temperature |
| DPS3 | Edgetech Instruments | Dew-point hygrometer |
| ACT-3X/ROLS-W | Monarch Instrument | Optical tachometer (fan speed) |
| IMFA0035 | Red Lion | Frequency counter (compressor speed) |
| DCT-0010-005 | Aim Dynamics | Current transducer (defrost on/off detection) |
| Baratron 220D | MKS Instruments | Barometric pressure |

3 Experimentation Plan

This section describes experimentation approach and the methodology used to develop equipment performance curves for EnergyPlus simulation platform. Enhancing the EnergyPlus building simulation library with performance data of the test article was the primary driver for developing the experimentation plan. EnergyPlus models simulate building and HVAC performance in various climates by using short (typically 15-minute) timesteps integrated into hourly and annual predictions. The simulations account for dynamic hourly interactions between building thermal loads, equipment performance, and weather. Simulation outputs include but are not limited to energy consumption, electric demand, building heating and cooling loads, and equipment capacity.

Performance mapping the heat pump over a wide variety of psychrometric conditions will provide the required model inputs to simulate annual building energy consumption. During performance mapping, obtaining performance data across a wide range of independent variables is more important than the need to gather data at any specific test condition. Wide ranges of data collection ensure that the developed performance regressions used to underpin the EnergyPlus model remain valid even during extreme design heating/cooling days.

The following subsections describe the systematic approach followed in the project to develop performance mapping of the equipment:

Section 3.1: Run the test article under varying conditions to better understand its embedded controls and operational limits.

Section 3.2: Develop a design of experiment that vary critical parameters and characterizes the equipment performance over its expected range of operation.

Section 3.3: Adjustments required to transform the high-altitude data to heat pump performance at sea level conditions.

Section 3.4: Characterize the equipment performance at each of the design of experiment conditions.

Section 3.5: Curve fit the performance data into regression models to extrapolate between test conditions.

3.1 Embedded Controls and Limits of Operation

The performance of vapor compression air conditioning (and heat pump systems) varies continuously depending on the sensible (temperature) and latent (humidity) loads on the indoor and outdoor units. Traditional, constant-speed, split air-conditioning systems operate the compressor, outdoor, and indoor fans at full speed when providing heating or cooling, despite the building's varying thermal load. These units undergo frequent on/off cycling to meet the thermostat setpoint. The on/off cycling maintains a building temperature that oscillates significantly above and below the temperature setpoint.

Variable-speed systems can modulate the indoor fan, outdoor fan, and the compressor to match the equipment capacity to the varying building loads. As a result, these units run continuously while using the minimum amount of power to provide heating or cooling. This strategy provides superior levels of comfort due to negligible space temperature fluctuations and energy savings over traditional single-speed HVAC systems.

Variable-speed systems have numerous sensors and embedded controls to optimize the efficiency and performance. The controls also ensure equipment longevity by limiting the operational ranges within the physical constraints of the equipment. Understanding these boundaries is essential to properly design an experimentation matrix that allows for data collection over a wide range of conditions within the operational range of the equipment.

3.1.1 Variable-Speed Compressor

Performance mapping a constant-speed system requires monitoring system operation as a function of varying indoor/outdoor temperatures and humidity conditions. This requirement is equivalently applicable to performance mapping variable-speed systems; however, the evaluation is more extensive due to the complexity of determining the conditioning capacity and performance at various compressor speeds. As the building's heating or cooling load changes, the heat pump modulates its compressor speed to match the space-conditioning needs.

Prior to developing a design of experiment, the equipment was run over a wide range of conditions to determine the operating boundaries. This ensured the broad range of test points were within the operational limits. Laboratory observations and measurements determined the

minimum and maximum compressor speeds are primarily limited as a function of the outdoor air temperature. This is sensed by a thermistor mounted on the outdoor unit. Additionally, in heating mode, the thermostat setting (comfort or efficiency mode) puts secondary limits on the maximum compressor speed.

Although the system can operate beyond the outdoor temperatures plotted in Figure 7 and Figure 8, it represents the temperature range of the test matrix. In cooling mode, the compressor minimum and maximum speed limits are the same for comfort mode and efficiency mode. In heating mode, the minimum compressor speeds are the same for comfort mode and efficiency mode, but the two modes have different maximum compressor speed limits, as shown in Figure 8.

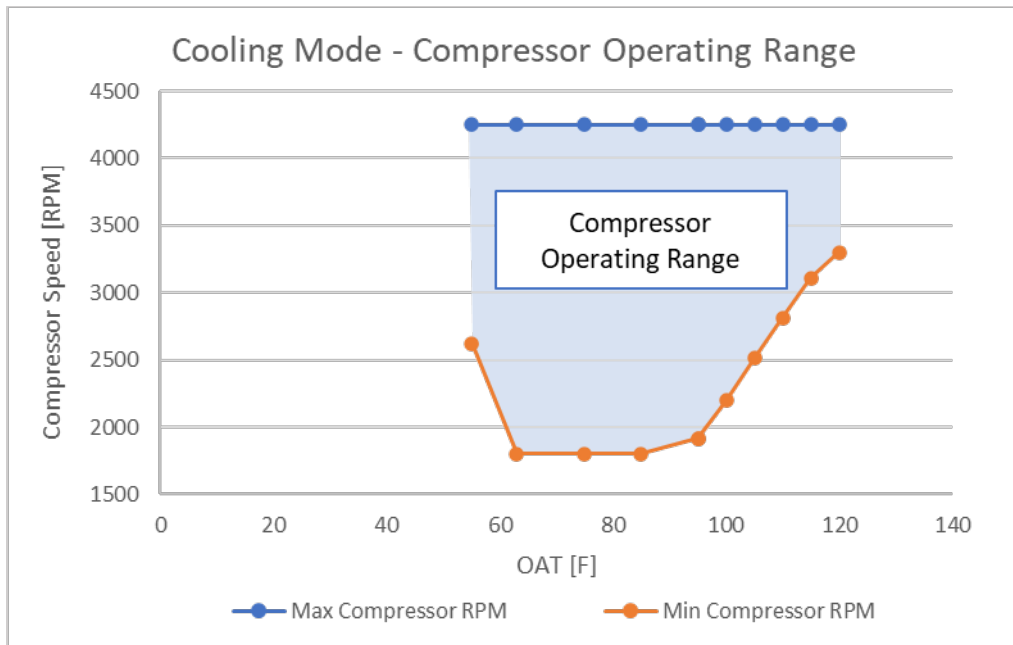


Figure 7. Variable speed limits when the compressor operates in cooling mode

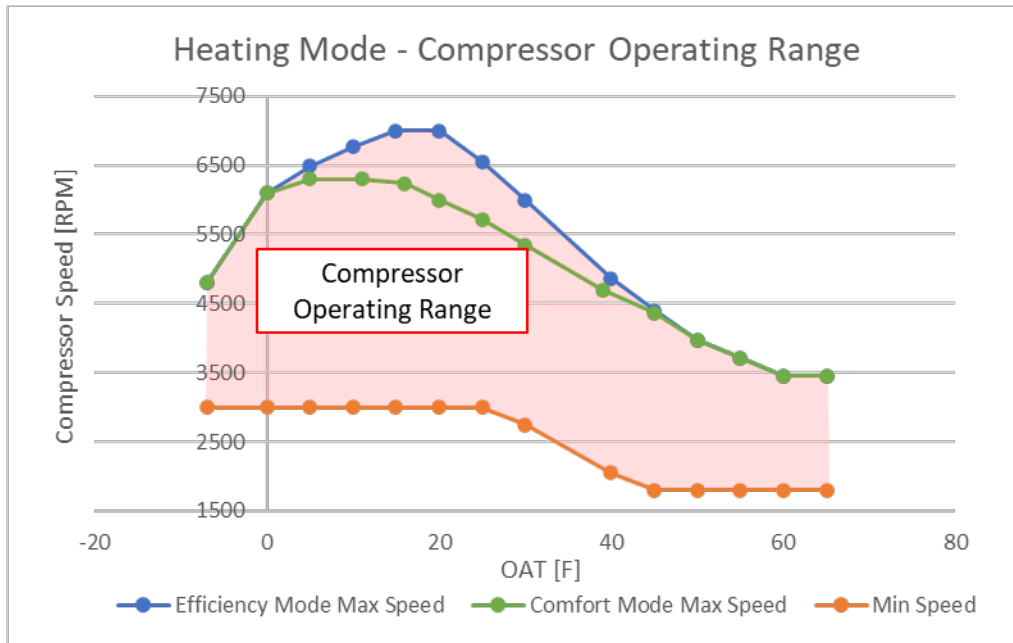


Figure 8. Variable speed limits when the compressor operates in heating mode

3.1.2 Thermostat Modes

The heat pump thermostat can operate the equipment in four general modes: technician checkout, comfort, efficiency, and maximum. Depending on the thermostat mode, the indoor unit fan speeds are controlled differently as the compressor speed varies. These differences in the thermostat’s mode of operation have implications on the exiting supply air state, the conditioning capacity, and energy consumption.

Technician checkout mode is required on all variable-speed HVAC equipment. This is primarily used for third-party AHRI 210/240 (AHRI 2023) test rating and certification (SEER and HSPF). In this mode, a technician can force the unit to operate at a user-specified compressor speed between 50% and 100% of full capacity. The indoor fan speed operates according to the capacity setting. Although this mode of operation provides the easiest means to modulate the compressor speed during testing, it is unclear if this mode of operation represents the heat pump’s behavior under the other three “normal” thermostat control modes. While the project initially observed and compared the heat pump operation in technician checkout, comfort, and efficiency modes, it was concluded that the results were difficult to interpret due to inconsistency in the equipment operating speeds under various indoor and outdoor temperatures. To characterize the equipment most accurately in its typical modes of operation, both comfort and efficiency modes were evaluated separately to capture performance differences.

Comfort mode is the default thermostat setting. As implied, the heat pump operates to prioritize occupancy comfort. When set to provide cooling, the air-handler fan speed operates at a relatively low flow per thermal capacity (cfm/ton), which provides better dehumidification. The thermostat measures and considers both the space temperature and indoor humidity when determining the supply air flow rate. The range of air-handler unit flow rates for the two modes of operation can be seen in Figure 9.

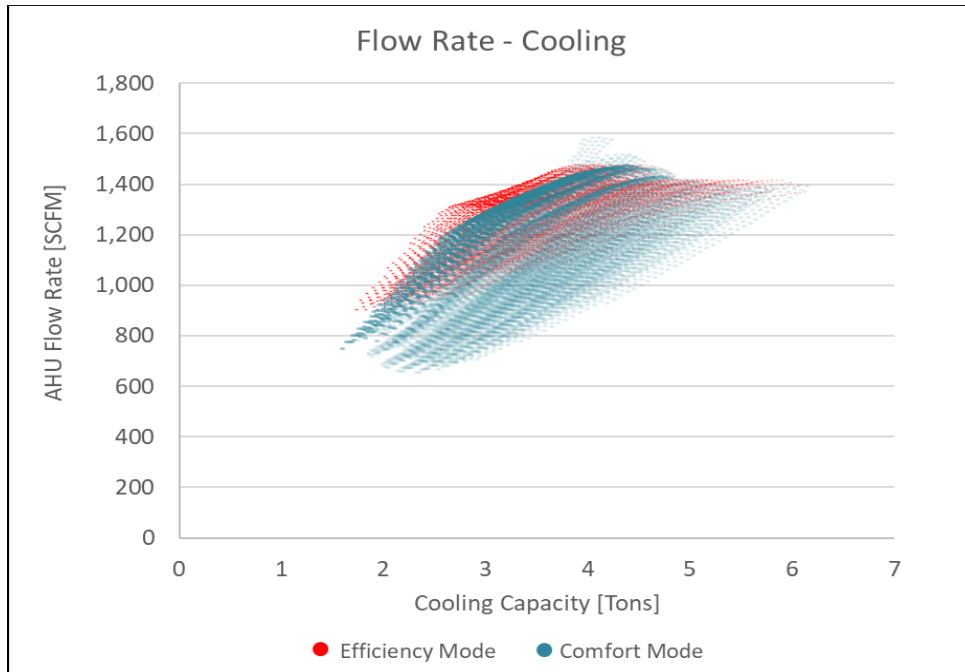


Figure 9. Air-handler unit flow rates for two modes of cooling operation; data points represent the performance lookup table generated across a broad range of indoor and outdoor conditions

Although additional thermostat settings are available to provide further dehumidification control, these were not adjusted, and the default values were used. When the heat pump is set to provide heating in comfort mode, the humidity measurement is neglected. During heating, comfort mode maintains lower air-handler unit flow rate to provide a higher supply air temperature than in efficiency mode (Figure 10). Independent of the mode of operation and under extremely cold outdoor air temperatures, the heat pump will require auxiliary heating due to the dramatically lower supply air temperatures (Figure 11).

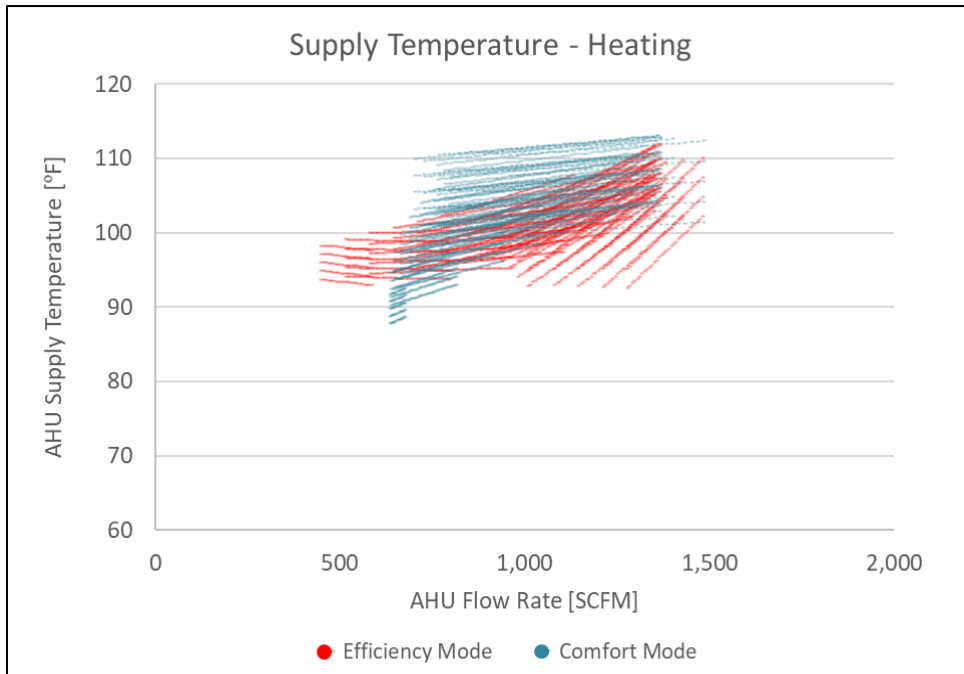


Figure 10. Air-handler unit supply air temperature for the two modes of heating operation; data points represent the performance lookup table generated across a broad range of indoor and outdoor conditions

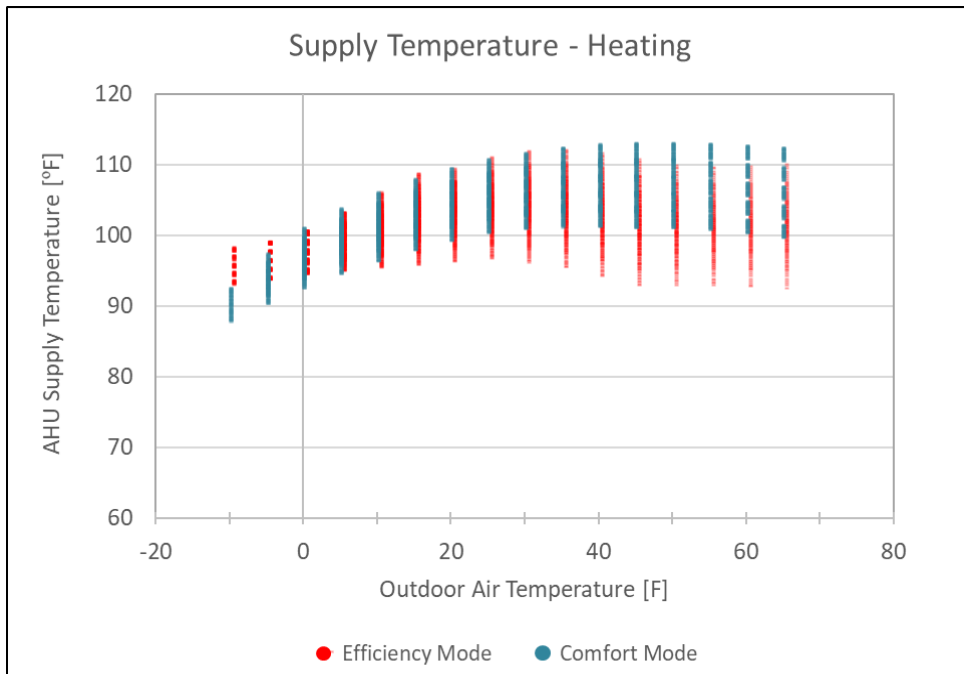


Figure 11. Supply air temperatures with respect to the outdoor air temperature and mode of operation based on the performance lookup table

Efficiency mode operates the equipment to prioritize energy savings. During space cooling, a faster fan speed increases the sensible heat ratio (SHR) such that sensible efficiency is improved, but at the detriment of latent capacity. When providing space heating, a faster fan speed improves heating efficiency but reduces supply air temperature, which some people perceive as uncomfortable. Figure 8 also shows that the compressor can operate at higher speeds. This boost in capacity allows the outdoor unit to extract more heat from the outside air, presumably at increased efficiency.

Because the focus of the project was to ascertain the energy efficiency benefits of the test article, we decided to eliminate the max mode (fourth mode of operation) from the experimentation plan. Additionally, this low-priority evaluation would have increased the number of experimentation permutations and complexity.

All other thermostat settings remained as the factory default values. Additional information on the numerous functions, settings, and features of the thermostat (SYSTXCCITC01-B) can be found by referencing the user manual.

3.2 Design of Experiment

Performance mapping the heat pump requires a wide combination of factors to be varied. These independent variables affect the equipment capacity and energy consumption. Due the vast number of combinations that result from the independent variables, a full-factorial test matrix would not be practical. Instead, the use of a statistical software package, JMP[®] from SAS[®], was used to develop a custom design of experiment. The software determines a test matrix, guided by classical design of experiment principles, which significantly reduces the number of test combinations needed to develop low-uncertainty response surface methodology regressions. The independent inputs and specified ranges needed to develop the cooling and heating test matrix are explained in the following sections.

3.2.1 Cooling Mode

The factors that affect the capacity, performance, and energy consumption of a heat pump in cooling mode are the outdoor dry-bulb air temperature, the indoor dry-bulb return air temperature, the indoor return air wet-bulb air temperature (humidity), and the speed of the compressor and fans.

Instead of specifying the indoor humidity as a wet-bulb temperature, the test matrix captures this factor using dew-point depression. The dew-point is a measure of the absolute humidity or water vapor present in the air. The dew-point depression is a delta temperature that is subtracted from indoor dry-bulb temperature, resulting in the dew-point temperature.

Two designs of experiments were developed to characterize the indoor unit under high humidity (relatively small dew-point depressions) and low humidity (large dew-point depressions) conditions. These tests are respectively designated as a wet-coil conditions and dry-coil conditions. The wet-coil conditions assess the performance of the system when the indoor unit provides both latent (dehumidification) and sensible cooling. Under these conditions, water vapor is removed from the air and condensate forms on the cooling coils. The dry-coil conditions assess the indoor coil performance when no dehumidification occurs. When the dew-point depression is sufficiently large, the moisture content of indoor air is very low. Under these

conditions, dehumidification cannot occur because the evaporator coil temperature is above the indoor airstream dew-point. This results in a system that provides exclusively sensible cooling capacity.

Last, the operation of the unit in comfort mode and efficiency mode were also characterized. This again doubled the number of tests performed to provide an extensive understanding of the equipment performance. The factors and the specified range for which the design of experiment was developed to performance map the heat pump in cooling are shown in Table 7. The explicit matrix of wet-coil and dry-coil test conditions can be found in Table 14 and Table 15 in the Appendix.

Table 7. Factors and Ranges Specified to Develop the Cooling Design of Experiment Test Matrix

| Independent Variable | Type of Variable | Range: Wet-Coil | Range: Dry-Coil |
|--|---------------------|---------------------|---------------------|
| Outdoor dry-bulb air temperature | Continuously varied | 55° to 120°F | 55° to 120°F |
| Indoor return air dry-bulb temperature | Continuously varied | 68° to 82°F | 68° to 82°F |
| Indoor return air dew-point depression temperature | Continuously varied | 5° to 25°F | >35°F |
| Compressor speed ⁴ | Continuously varied | 1,850 to 4,250 RPM | 1,850 to 4,250 RPM |
| Thermostat mode | Discretely varied | Comfort, efficiency | Comfort, efficiency |

⁴ The compressor speed is bounded by its operational limits shown in Figure 7.

3.2.2 Heating Mode

The factors that affect the capacity, performance, and energy consumption of a heat pump in heating mode are the outdoor dry-bulb air temperature, the outdoor wet-bulb temperature (humidity), the indoor dry-bulb return air temperature, and the speed of the compressor and fans.

In heating mode, the air-handler indoor coil acts as the refrigerant condenser where the superheated, high-pressure, refrigerant gas exchanges heat with the space return air blowing over the coils. The coils of the outdoor unit act as the evaporator where the expansion of high-pressure liquid refrigerant extracts heat from the outdoor air. Depending on the outdoor moisture content, frost formation can occur on the outdoor coil when the saturated refrigerant temperature is lower than the outdoor air dew-point. Under these conditions, the water vapor from the air freezes on the outdoor coil resulting in degradation of heat transfer.

Consequently, elimination of frost is important to maintain heat transfer effectiveness across the outdoor coil. Therefore, periodically the unit initiates defrost cycles, which temporarily reverses the operation of the equipment similar to a cooling cycle. At outdoor temperatures below 50°F, the heat pump enables defrost cycles to keep the outdoor coil free of frost and ice. Although the defrost cycle is essential for reliable heating operation, this poses two detrimental impacts: 1) energy is consumed to defrost the coil instead of heating the building, and 2) heat already supplied to the space by the heat pump is removed from the building and used to defrost the outdoor coil. This results in cold air being blown through the building supply ducts.

A defrost cycle can last between 3.5 and 10 minutes. During this time, heat from the space is absorbed in the refrigerant through the indoor unit coil and rejected to the outdoor coil to melt the frost. This is a parasitic process that removes heat from the indoor space and uses the heat pump energy solely to melt the ice. The defrost cycle frequency and duration are dependent on the thermostat settings. By default, the system is set to defrost “automatically.” Detailed information related to the manufacturer’s automatic defrost control logic and the defrost time intervals can be found in Figure 27 in the Appendix.

Elevated outdoor dew-point temperatures result in frost formation and frequent defrost cycles which add complexity to steady-state performance mapping the system in heating mode. Two designs of experiments were developed to characterize the heating performance. The first test was designed to assess the heating capacity and energy consumption of the heat pump under (relatively) frost-free conditions. The second test was designed to analyze the heating capacity and COP degradation over long operating periods of operation. Through these experiments, the performance degradation due to frost formation was characterized and energy penalty from defrost cycle was quantified.

The heat pump performance was first characterized under low humidity conditions during which the coil developed minimal frost. The goal was to replicate a dry-coil, steady-state heating test when no dew (or frost) would form on the outdoor unit coils. To minimize defrost cycle interruptions and allow sufficient time for steady-state performance to be achieved, the thermostat defrost setting was increased to the maximum, 120-minute, time interval. Additionally, no humidity was added to the test chamber via the laboratory air streams, which reduced the rate of frost buildup. Because these tests were performed during the month of April in Golden, Colorado, the makeup air dew-point supplied by the laboratory naturally ranged from -12°F to -4°F. This imposed the lowest humidity conditions achievable on the outdoor unit. Minimizing the humidity levels during testing represents the highest achievable, steady-state performance data due to a dry and frost-free coil.

The variables and ranges for which this design of experiment was developed to characterize the heating performance are shown in Table 8. Not all combination of the ranges could be reached in the environmental chamber. For example, the -7°F outdoor air condition created inside the test chamber was only achievable at the maximum compressor speed and the minimum indoor return-air temperature. The explicit matrix of steady-state test conditions can be found in Table 16 in the Appendix.

Table 8. Factors and Ranges Specified to Develop the Steady-State Heating Design of Experiment Test Matrix

| Independent Variable | Type of Variable | Range |
|--|---------------------|---------------------|
| Outdoor dry-bulb air temperature | Continuously varied | -7° to 60°F |
| Indoor return air dry-bulb temperature | Continuously varied | 60° to 76°F |
| Compressor speed ⁴ | Continuously varied | 1,800 to 7,000 RPM |
| Thermostat mode | Discretely varied | Comfort, efficiency |

⁴ The compressor speed is bounded by its operational limits shown in Figure 8.

A second set of tests was performed to better understand the heating capacity degradation and increased energy use as frost forms. These tests operate the heat pump at the minimum or maximum heating capacity, at a constant outdoor air temperature and high humidity levels, for extended periods of time (8 to 12 hours). Over time, as frost accumulates on the coil, the heat transfer effectiveness decreases. The gradually decreasing heating capacity results in longer compressor runtimes to meet the thermostatic setpoint. Integrating the degrading heating capacity and varying energy usage between and during defrost cycles characterizes an average capacity and COP. The heating performance under defrost periods was compared with the ideal steady-state, dry-coil performance to estimate degradation factors. All tests were run with the thermostat set in comfort mode with the assumption that the derating factors, based only on compressor speed and outdoor air temperature, can be applied in efficiency mode. During these experiments, the thermostat was programmed to the default “Auto” defrost setting. The automatic defrost control logic is explained in the Carrier service manual and included in Figure 27 in the Appendix.

3.3 Testing Adjustments and Measured Performance Corrections

Equipment performance at sea level conditions is desired for EnergyPlus simulations. The lower air density due to NREL’s location at 5,865 feet above sea level skews the experimental results. Therefore, corrections were made during experimentation and during data postprocessing to adjust the measured performance at altitude to what is expected at sea level. The following sections will discuss those adjustments.

3.3.1 Outdoor Unit Fan Flow

The axial fan on the outdoor unit of the heat pump is driven by an electrically commutated motor (ECM) to provide variable-speed fan operation. The volumetric flow rate drawn through the outdoor unit coils by the fan is directly proportional to its rotational speed. The volumetric flow rate versus fan speed is correlated from measurements taken by the averaging pitot tube array and an optical tachometer. From this relationship, the volumetric flow rate is known solely based on the fan speed.

The lower ambient air pressure experienced at altitude results in lower air density. For the same volumetric flow rate at sea level, the lower air density at altitude results in approximately 20% less mass flow rate through the outdoor coil. Therefore, the mass flow rate of the thin-air through the test article must be increased to ensure an equivalent heat transfer rate at sea level. This is accomplished by assisting the outdoor unit fan and drawing additional volumetric flow through coils using the environmental chamber booster fan. The outdoor fans volumetric flow rate, correlated to its rotational speed in RPM, is boosted dynamically during testing by the ratio of the ambient air pressure (or density) at sea level and altitude expressed in Equation 1.

$$\dot{V}_{SL} = \dot{V}_{alt}(RPM) * \frac{P_{amb,SL}}{P_{amb,alt}} \quad (1)$$

This correction was applied to all steady-state cooling tests. The flow boost was also applied to the steady-state heating tests at outdoor air temperatures above 18°F. Temperatures lower than 18°F showed no additional heat transfer rate when the flow was increased, and no air mass flow boosting was applied.

3.3.2 Outdoor Unit Fan Power

The lower density air results in reduced electrical fan power measurements at altitude. To properly account for the overall efficiency of the heat pump at sea level, corrections to the measured electrical fan power must be adjusted when postprocessing the data.

The outdoor unit hydraulic fan power and power consumption are governed by the volumetric air flow rate, the static pressure, and the fan/motor efficiency. The volumetric flow rate is a function of the fan speed. However, at sea level, the fan power will increase as more static pressure is imposed on the fan due to the denser air. Assuming a constant fan/motor efficiency, the fan power (measured under thin-air conditions) can be adjusted by the ratio of the ambient pressures of sea level and altitude. Prior to running performance tests, a correlation was developed to characterize the (thin-air) electrical power consumption of the outdoor unit fan versus the fan speed. The measurements, shown in Figure 12, were taken using an Acuvim power meter and an optical tachometer. Identical measurements were also taken in heating operation, which generated a slightly different correlation.

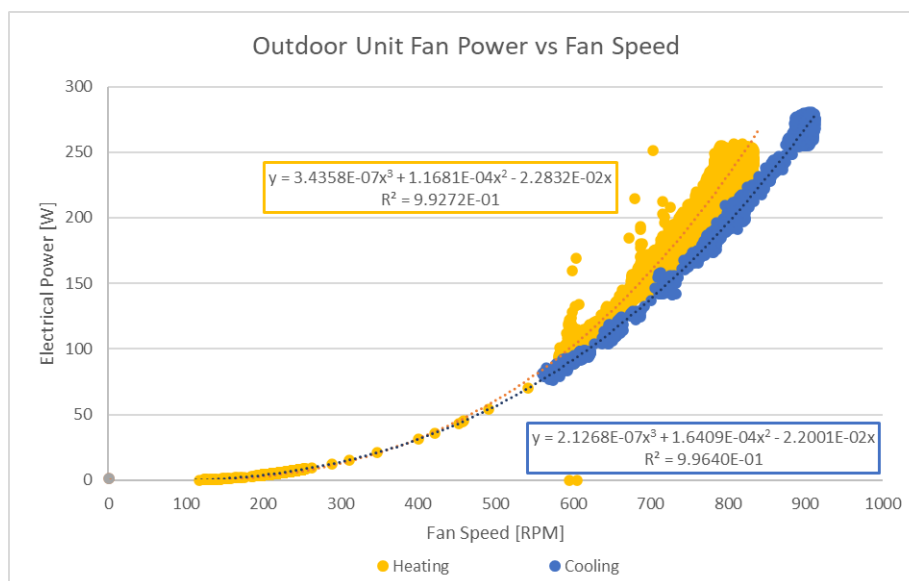


Figure 12. Electrical power consumption of the outdoor fan unit relative to fan speed

All steady-state performance data were postprocessed to apply the fan power corrections and adjust for sea level air density. Also shown in Figure 12, the expected outdoor fan power in cooling and heating operation are represented by the empirical equations 2 and 3 below. The measured fan power during testing was subtracted from the total system power and the corrected fan power substitutions were added.

$$\dot{Q}_{fan,SL} = [(2.127 * 10^{-7}) * (RPM)^3 + (1.641 * 10^{-4}) * (RPM)^2 - (2.200 * 10^{-2}) * (RPM)] * \frac{P_{amb,SL}}{P_{amb,alt}} \quad (2)$$

$$\dot{Q}_{fan,SL} = [(3.436 * 10^{-7}) * (RPM)^3 + (1.168 * 10^{-4}) * (RPM)^2 - (2.283 * 10^{-2}) * (RPM)] * \frac{P_{amb,SL}}{P_{amb,alt}} \quad (3)$$

3.3.3 Indoor (Air-Handler) Fan Power

The air-handler fan, driven by an electrically commutated motor, varies the fan speed to meet a predetermined standard volumetric flow. This is based on the equipment's operating heating or cooling capacity, a user altitude input in the thermostat, and the measured external static duct pressure imposed on the fan. The controls calculate and set the fan speed to deliver the exact standard cubic feet per minute of air flow knowing the manufacturers fan curves and monitoring the current draw. The flow rate can be displayed on the thermostat and the accuracy over a wide range of operation was confirmed to be within a few percent of the laboratory nozzle measurements. Whether at altitude or sea level, the system attempts to supply a standard volumetric flow rate. Two adjustments are made to accurately represent indoor unit fan power under testing.

The first adjustment is imposed dynamically during evaluation. The AHRI 210/240 (AHRI 2023) specifies that the air-handler must experience a maximum external static pressure (ESP) of 0.5 inches of water column (w.c.) at the maximum volumetric flow rate. This imposed resistance represents the fan power consumption as if it were installed in a ducted system at sea level. As the air-handler modulates to lower flow rates, the maximum ESP imposed on the fan is reduced by equation 4. The pressure imposed across the air-handler is measured by laboratory and adjusted with the laboratory inlet and exhaust fans.

$$\Delta P_{static, reduced\ flow} = \Delta P_{static, max\ flow} * \left(\frac{P_{amb, SL}}{P_{amb, alt}} \right) * \left(\frac{\dot{V}_{reduced\ flow}}{\dot{V}_{max\ flow}} \right)^2 \quad (4)$$

The second adjustment is performed when postprocessing the data to correct the measured electrical fan power to represent sea level conditions. For the air-handler to move the proper standard volumetric flow of air at altitude, the fan must spin faster to push more volume of the less dense air. The fan consumes more power by operating at higher speeds to move more of the less dense air and meet the standard volumetric flow rate requirement. The additional flow compounds further energy consumption, due to the higher internal static pressure generated across the cooling coil. Therefore, the fan consumes more electrical power than it would at sea level from the multiple facets of higher flow and higher internal static pressure. The measured electrical fan power must be adjusted and reduced by a ratio of the ambient pressures squared, as shown in equation 5. This correction was applied when postprocessing the test data in cooling and heating operation.

$$\dot{Q}_{fan, SL} = \dot{Q}_{fan, alt} * \left(\frac{P_{amb, alt}}{P_{amb, SL}} \right)^2 \quad (5)$$

3.3.4 Sensible Heat Ratio (Cooling Only)

The total cooling capacity is composed of sensible and latent components. Sensible heat ratio is the ratio of sensible cooling to total cooling (sensible and latent). A sensible heat ratio of one represents a dry, indoor coil.

Under dry-coil test conditions, no dehumidification can occur. Therefore, the total cooling capacity goes exclusively to sensible cooling. For the identical refrigerant flow rate (or

compressor speeds), no sea level cooling capacity corrections are required to adjust the data measured at altitude if a few conditions are met. The first condition is the air mass flow rate at altitude and sea level through the indoor and outdoor coil are equal. The second condition is that the inlet dry-bulb temperature and relative humidity stay the same. If these conditions are met, the dry-coil efficiency is identical between sea level and altitude because the effectiveness of a sensible, finned coil heat exchanger is solely dependent on the number of transfer units.

During wet-coil evaluation, mass transfer occurs when water vapor from the moist air stream condenses on surface of cold coil. Under wet-coil test, the sensible heat ratio requires a minor altitude adjustment to accurately represent the coil outlet conditions at sea level. The sensible and latent performance is adjusted by means of calculating the sea level supply air conditions that provide the same capacity and relative humidity as the test result (at altitude). This method maintains equal number of transfer units of the evaporator coil. This is also explained by Wheeler et al. (2018).

3.4 Characterizing the Equipment Performance

The test article was evaluated for cooling and heating performance under its two inherent control modes of operation—comfort and efficiency. As the temperature and humidity conditions vary, the unit will modulate the compressor speed, and outdoor and indoor fan speeds to provide appropriate space conditioning. The outdoor unit senses the ambient outside temperature while the thermostat measures the indoor space temperature and humidity. The controls programmed into the thermostat account for these factors to adjust the system speeds at a 1-minute interval. As the heat pump capacity modulates, the laboratory connected to the environmental test chamber responds accordingly to maintain constant conditions during experimentation. The execution of operating the laboratory and collecting the data will be described in the following sections.

3.4.1 Steady-State Cooling Mode Tests

The laboratory supplies the air at the desired test conditions to the indoor unit that represent a “return air” temperature and humidity. Air flow and pressure is also maintained across the indoor unit to maintain a prescribed external static pressure representative of ductwork per AHRI 210/240 (AHRI 2023). As the indoor unit fan changes speed, the laboratory controls dynamically adjust using a proportion, integral, derivative algorithm to maintain the proper setpoints.

The outdoor unit rejects the heat from the refrigerant to the air inside of the environmental chamber. The laboratory fans exhaust a small portion of the hot air and supply cool makeup air back into the chamber to ensure the environmental chamber air temperature remains constant during experimentation. Through a set of air flow dampers on the environmental chamber, the cool makeup air mixes with the outdoor unit’s exhaust air to maintain the desired temperature setpoint. The booster fan recirculates the mixed air back to the inlet of the heat pump. Also, the booster fan speed, which is controlled by the laboratory, draws additional air through the outdoor unit to provide air mass flow rates equivalent to sea level conditions.

The test article makes compressor speed adjustments once per minute based on the temperature deviation between the space temperature and the thermostat’s setpoint. As the space temperature deviates further from the setpoint temperature, the thermostat communicates with the indoor and outdoor units to increase the cooling capacity. The heat pump will speed up its compressor and

fans based on its embedded controls. As the space temperature approaches the setpoint, the thermostat will decelerate the system speed. The laboratory indirectly modulates the heat pump speed by connecting a signal to the thermostat, which emulates a remote room temperature sensor. This signal becomes the primary space temperature input to which the thermostat reacts. The laboratory uses a feedback control loop that varies the emulated space temperature signal until the compressor speed matches the desired compressor setpoint value (Figure 13).

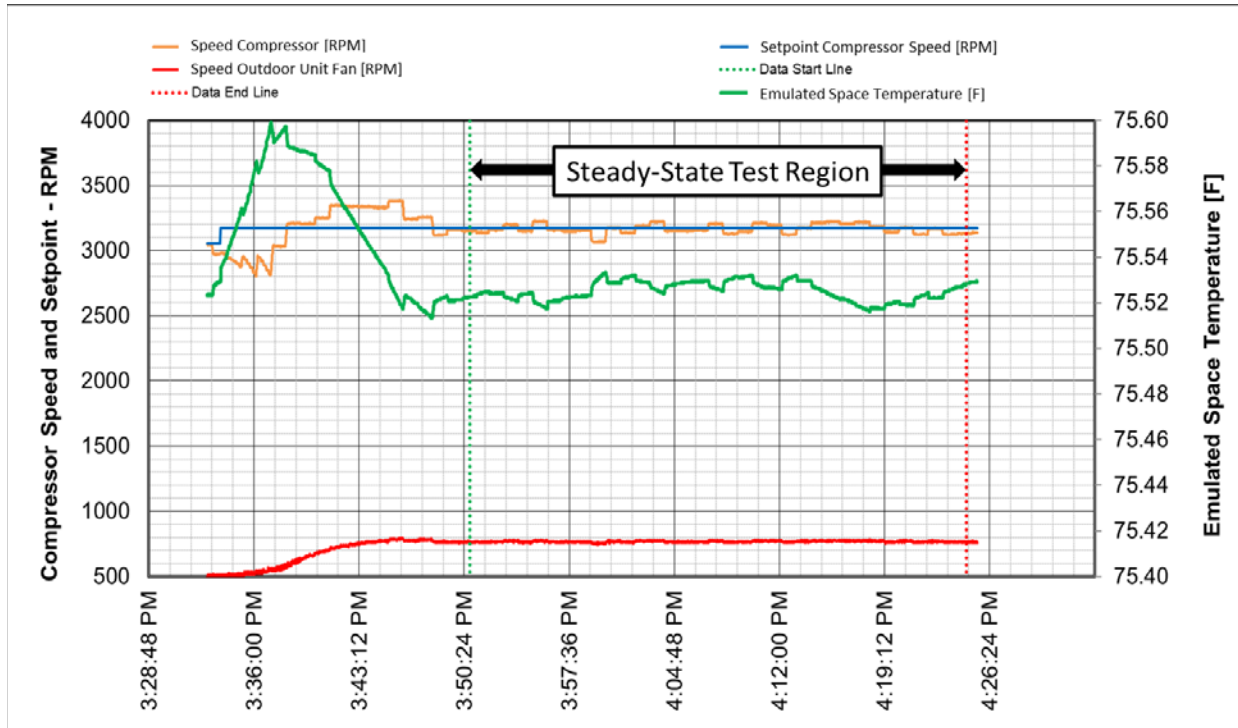


Figure 13. Controlling the compressor speed by emulating a room temperature signal on the thermostat

The thermostat monitors humidity as the secondary input for controlling the indoor unit fan. The humidistat is a small sensing chip built onto the control board of the thermostat. During experimentation, the thermostat was mounted in the return air plenum such that the thermostat could sense the humidity entering the air-handler (Figure 14).

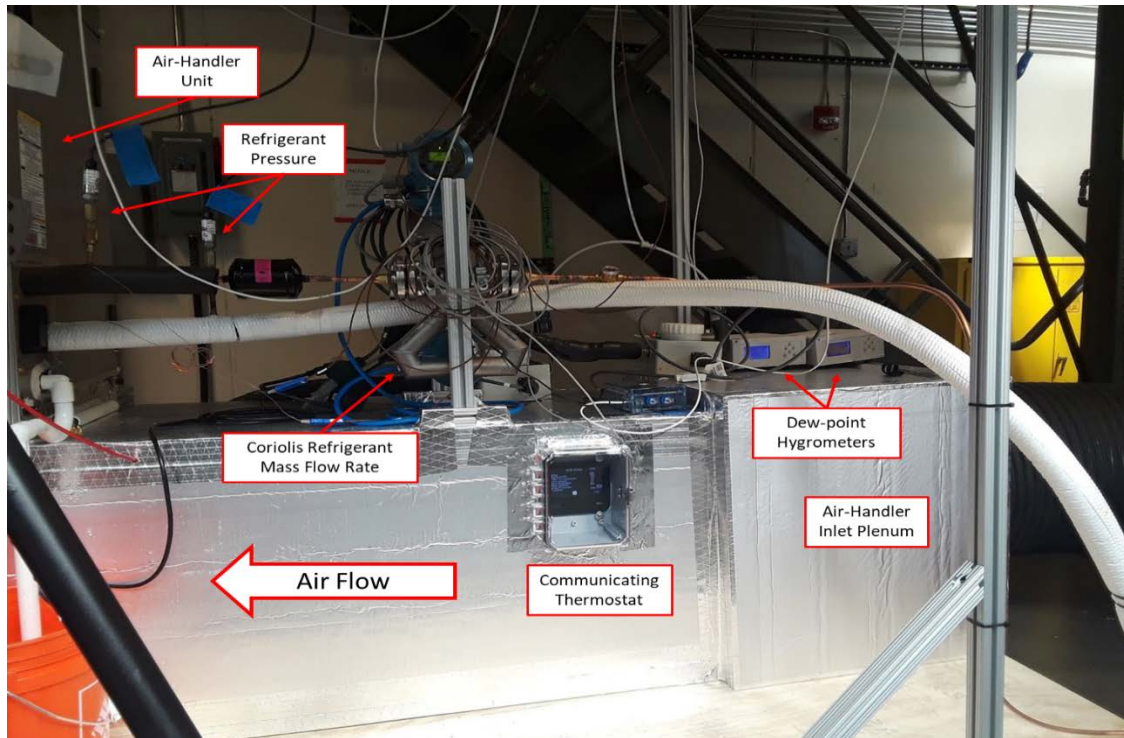


Figure 14. Thermostat and instrumentation on the indoor unit

During experimentation, steady-state conditions of the laboratory and the heat pump operation must be achieved before data collection. This is assessed by monitoring variables related to the air temperatures, dew-points, flow rates, and pressures as well as the heat pump compressor speed, fan speeds, and the refrigerant pressures. Once steady-state operation has been reached, more than 200 data variables are collected once per second over a 20- to 45-minute interval. The data is then postprocessed to adjust for altitude effects. The test matrix containing the adjusted, postprocessed values for steady-state cooling performance can be found in Table 17 and Table 18 in the Appendix.

3.4.2 Steady-State Heating Mode Tests

The methodology and laboratory operation to characterize the unit in heating mode is similar to the approach for cooling performance characterization. Constant psychrometric inlet conditions are supplied to the indoor unit and the environmental chamber to reach steady-state operation. The laboratory senses and adjusts dynamically using feedback controls to maintain temperature, humidity, air flow, and pressure setpoints to the indoor and outdoor units.

In heating mode, the outdoor unit removes heat from the air inside of the environmental chamber. This process continuously cools the chamber to lower temperatures. The laboratory fans exhaust a small portion of this cold air and supply warm makeup air back into the chamber to ensure the chamber air temperature remains constant during testing. To maintain the desired temperature setpoint, the environmental chamber dampers modulate proportionally, which mixes the warm makeup air with the cold air exhausted by the heat pump. The booster fan recirculates the mixed air back to the inlet of the heat pump. It also draws additional air through the outdoor unit to provide air mass flow rates equivalent to sea level conditions. However, it was observed

that additional air mass flows at the colder temperatures had negligible effects on capacity and power, therefore at temperatures less than 18°F, air flow through the outdoor coil was drawn solely by the outdoor unit fan. The laboratory indirectly modulates the heat pump compressor speed similar to cooling mode. This is done by sending a control signal to the thermostat, which emulates a space temperature. In heating mode, the humidity measurements taken by the thermostat do not affect the operation of the system.

During steady-state tests, achieving equilibrium between the lab's environmental conditions and the heat pump operation is critical prior to data collection and performance analysis. In addition, the characterization must be conducted between defrost cycles and preferably with minimum frost formation on the coil. If a defrost cycle begins during a test, the chamber temperature rises, and the test must be restarted until steady-state conditions are re-established. Once steady-state operation has been reached, data collection begins. The data is then postprocessed to adjust for altitude effects. The test matrix containing the adjusted, postprocessed values for steady-state heating performance can be found in Table 19 and Table 20 in the Appendix.

3.4.3 Integrated Defrost Degradation Tests

A limited number of experiments were performed due to the long nature of the test to collect a single set of psychrometric conditions. These tests operate the heat pump over an 8- to 12-hour period where indoor and outdoor psychrometric conditions are held constant. The objective is to allow for heavy frost accumulation to ascertain performance degradation.

During defrost tests, the air-handler unit inlet condition was maintained at 68°F. This average return air temperature value was selected to minimize the number of independent variable test combinations. The outdoor unit was exposed to high humidity conditions inside the environmental chamber with a dew-point depression of only 2°F below the dry-bulb temperature. The environmental chamber's dry-bulb temperature was varied from 7°F to 40°F, and the system was operated either at the minimum or maximum compressor speed.

The compressor speed during defrost is solely dependent on the outdoor air temperature and is independent of comfort or efficiency mode setting. The defrost compressor speeds were measured at 3,850, 4,450 and 5,350 RPMs (Figure 15). The heat pump terminates the defrost cycle under one of two conditions:

1. If the outdoor air temperature is warmer than 25°F, defrost ends when the outdoor coil temperature sensor rises above 60°F
2. If the outdoor air temperature is below 25°F, defrost ends when the outdoor coil temperature sensor rises above 45°F.

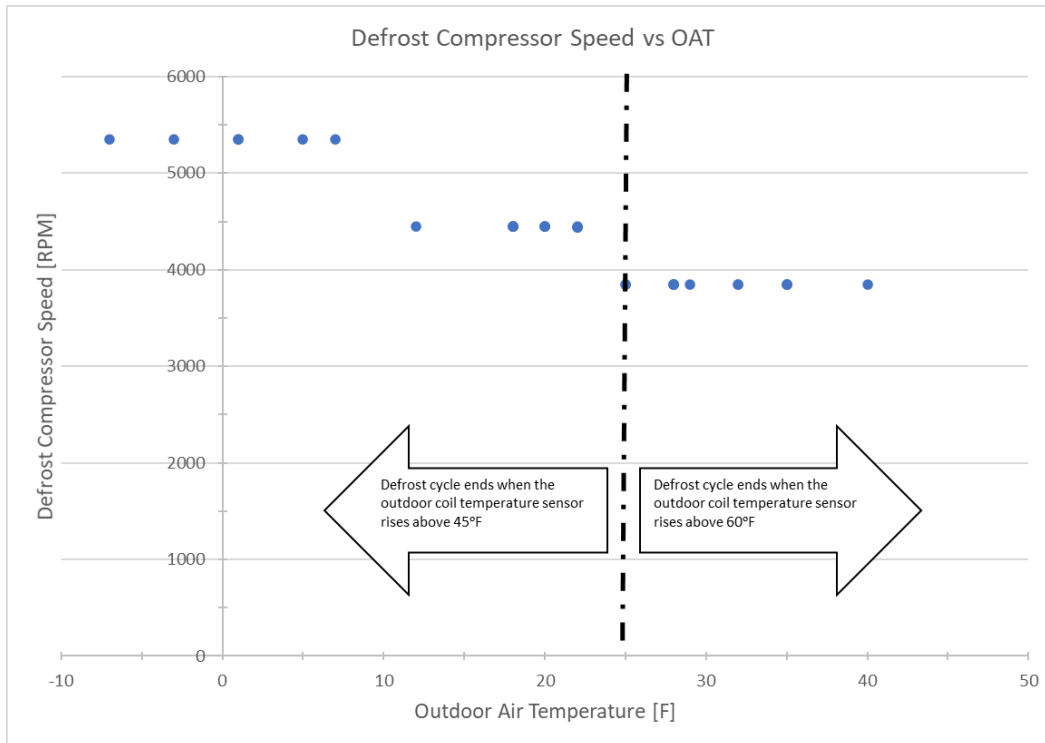


Figure 15. Compressor speed during the defrost cycle as a function of the outdoor air temperature

For all defrost tests, the environmental chamber booster fan was not used to boost the air mass flow through the outdoor unit coil. Because the booster fan only assisted in recirculating the air around the test chamber, the reduced volumetric air flow from frost accumulation could be measured. Also, during all defrost cycle tests, the thermostat was set to the default, “Auto,” defrost time interval. When set to “Auto,” the test article identifies a defrost need only when the outdoor air temperature is below 50°F, and the outdoor unit coil (surface) temperature is below 32°F. If these conditions are met, a timer limits the heating cycle run time to 30, 60, 90, or 120 minutes. The heating run time interval is based on the amount of time the prior defrost cycle ran. The less time required to defrost the outdoor coil, the more time the heat pump will spend running the following heating cycle. The corollary is also true such that if longer time is needed to defrost the outdoor coil, the heat pump will operate the subsequent heating cycle for less time.

The 8-hour time series shown in Figure 16 contains seven defrost cycles and six heating cycles. Trend lines of the heating capacity degradation, reduced air flow, the electrical power, and gross COP show the system performance as frost accumulates and how the amount of time spent in defrost dictates the following heating cycle time interval. The first defrost interval lasts 4 minutes, while the following heating cycle operates for 90 minutes. During the longer heating cycle, abundant ice accumulation gradually degrades the heating capacity until another defrost cycle is triggered. A longer defrost interval of 7 minutes is required to thaw the ice. Due to the longer defrost time interval, the test article limits the subsequent heating cycle to run for 30 minutes. The manufacturer’s automatic defrost control logic is explained in further detail by referencing the service manual or Figure 27 in the Appendix.

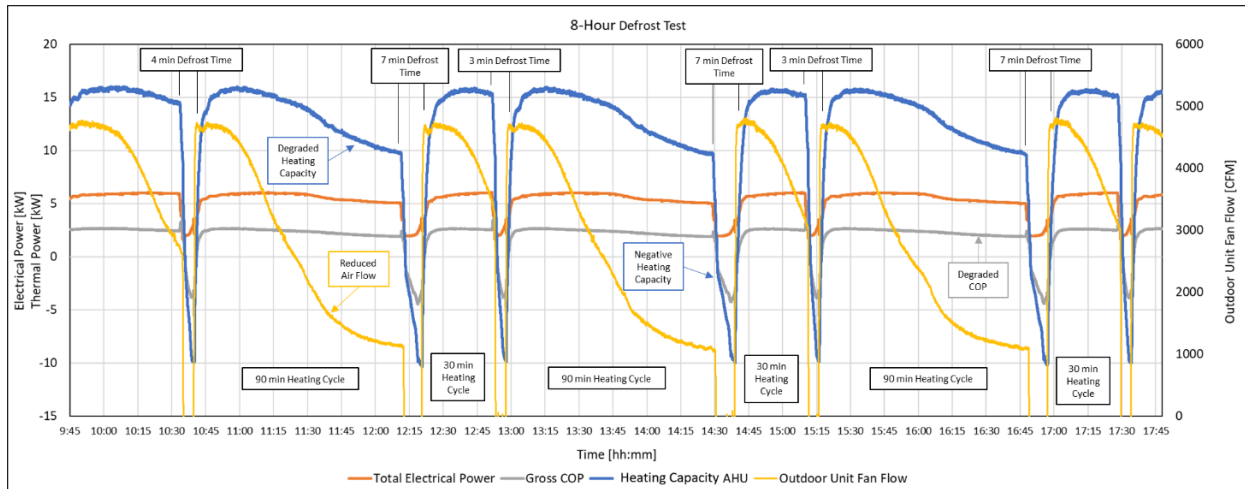


Figure 16. Defrost and performance degradation cycles over an 8-hour period maintaining an outdoor air temperature of 28°F

3.5 Regressing the Performance Data

The postprocessed data from Table 17 through Table 20 in the Appendix were used to compile performance prediction regressions. Each data table, representing comfort and efficiency mode, was treated separately. Furthermore, the dry-coil and wet-coil conditions in cooling mode were regressed independently. This resulted in a total of four sets of regressions that characterize cooling performance and two sets of regressions for heating performance. The varied test parameters and the postprocessed performance data were input into the statistical software package, JMP®. The software creates a second order, response surface methodology (RSM) model to empirically fit the postprocessed performance data relative to the independent variables. If any factors or cross terms in the regression were identified as statistically insignificant, they would be removed from the predictive model.

The RSM regressions are then used to develop an extensive lookup table that interpolates the heat pump capacity and performance to any permutation of parameters within the range of the test variables. The interpolated performance is used to provide EnergyPlus empirical predictions needed to simulate the heat pump annual energy consumption.

3.5.1 Steady-State Cooling Performance Regressions

The independent variables and the postprocessed tests were used to regress cooling performance parameters found in Table 9. The regressions are developed sequentially working from the top of the table down. The indoor, return air, wet-bulb temperature was used in these regressions as an independent variable derived from the indoor return air dry-bulb temperature and dew-point depression.

Using the empirical performance regressions, a lookup table was created for input into the EnergyPlus simulation environment. This table provides the predicted heat pump cooling performance parameters based on the compressor speed, outdoor dry-bulb air temperature, indoor dry-bulb return air temperature, and indoor return air wet-bulb temperature. When generating the lookup table, if the SHR was predicted to be a value of 1 or more, all dry-coil

performance regressions were substituted for the originally assumed wet-coil cooling performance.

Table 9. Independent Variables, Measured and Calculated Performance Values Used in the RSM Cooling Predictive Models

| RSM Performance Regressions | Factors Used in Regressions |
|--------------------------------------|--|
| Indoor standard volumetric flow rate | Compressor speed; Outdoor dry-bulb air temperature; Indoor return air wet-bulb temperature |
| Indoor external static pressure | Indoor standard volumetric flow rate |
| Air-handler, fan power | Indoor standard volumetric flow rate; Indoor external static pressure |
| Gross cooling capacity | Compressor speed; Outdoor dry-bulb air temperature; Indoor return air wet-bulb temperature |
| Gross sensible heat ratio | Compressor speed; Outdoor dry-bulb air temperature; Indoor return air dry-bulb temperature; Indoor return air wet-bulb temperature; Indoor standard volumetric flow rate |
| Gross COP | Compressor speed; Outdoor dry-bulb air temperature; Indoor return air wet-bulb temperature |

A comparison between the RSM cooling predictive regressions and the experimental data can be found in the Appendix. The performance regressions represent the mean predicted value with error bars that show the 2 sigma (U95) confidence interval. Figure 23 and Figure 24 show the quality of the fit relative to the data in comfort mode and efficiency mode, respectively. Predictions for the heat pump performance during simulation are kept within the ranges specified in Table 7 to eliminate unknown uncertainty and inaccuracy outside of the fit.

3.5.2 Steady-State Heating Performance Regressions

The independent variables and the postprocessed tests were used to regress heating performance parameters found in Table 10. The regressions are developed sequentially working from the top of the table down. The heating capacity was determined by assessing the sensible heating across the indoor coil after steady-state operations was reached and while the outdoor unit was performing under no or low frost conditions.

Using the empirical performance regressions, a lookup table was created for input into the EnergyPlus simulation environment. This table provides the predicted heat pump heating performance based on the compressor speed, outdoor dry-bulb air temperature, and indoor dry-bulb return air temperature.

A comparison between the RSM heating predictive regressions and the experimental data can be found in the Appendix. The performance regressions represent the mean predicted value with error bars that show the 2 sigma (U95) confidence interval. Figure 25 and Figure 26 show the quality of the fit relative to the data in comfort mode and efficiency mode, respectively. While the best practice is to test and regress the heat pump performance over the full range of simulated conditions, the tests were limited to a low outdoor air temperature of -7°F. Extrapolation of the performance regressions to an outdoor air temperature of -15°F were used in simulation because this is the manufacturer’s specified limit of the equipment’s operation.

Table 10. Independent Variables, Measured and Calculated Performance Values Used in the RSM Heating Predictive Models

| RSM Performance Regressions | Factors Used in Regressions |
|--|--|
| Indoor standard volumetric flow rate | Compressor speed; Outdoor dry-bulb air temperature |
| Indoor external static pressure | Indoor standard volumetric flow rate |
| Air-handler, fan power | Indoor standard volumetric flow rate; Indoor external static pressure |
| Gross heating capacity | Compressor speed; Outdoor dry-bulb air temperature; Indoor return air dry-bulb temperature |
| Gross COP | Compressor speed; Outdoor dry-bulb air temperature; Indoor return air dry-bulb temperature |
| Supply air temperature from the air-handler unit | Compressor speed; Outdoor dry-bulb air temperature; Indoor return air dry-bulb temperature |

Using the predictive performance regressions, the heating capacity and COP over a wide range of outdoor air conditions can be seen in Figure 17. The region represents the heating performance over the full range of compressor speeds at indoor return air temperatures between 68°F and 76°F. As the compressor speed decreases, the heating capacity decreases and the heat pump COP increases. As the indoor return air temperature increases, more compressor lift is required, so both the heating capacity and COP decrease.

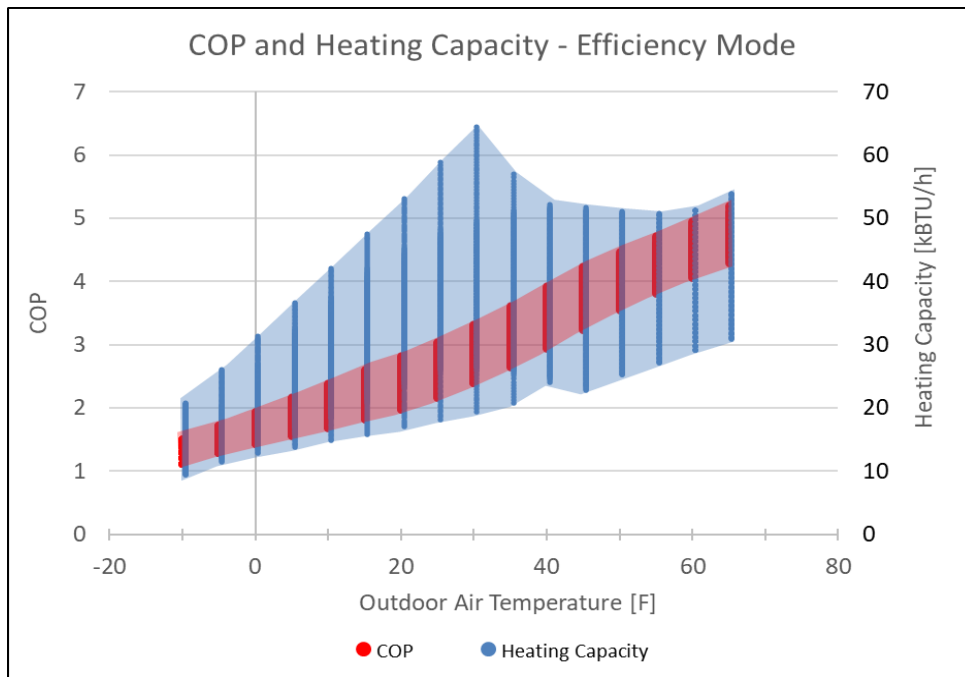


Figure 17. Expected range of varying heating capacity and COP versus outdoor air temperatures

3.5.3 Integrated Defrost Degradation Factor Regressions

Eleven tests were performed under high-humidity conditions to allow for multiple defrost cycles to occur during each test. Over the test period, the time varying heat capacity and COP was

analyzed and averaged. All values were adjusted for sea level corrections. The average performance over that period was compared with the predicted steady-state performance of the heat pump operating under low frost conditions. A ratio of the average, high-humidity performance to the maximum steady-state performance in a low-humidity environment provides a derating factor that allows an estimate of the system operation including defrost events. The derating factors are a fractional value between zero and one.

Multiplying the respective derating fractions to the idealized, low frost, steady-state performance provides an effective heating capacity and COP. The effective values capture the energy usage during the heating cycle, the defrost cycle plus the cooling effect (negative capacity) from the space that provides the heat to thaw the outdoor coil. The defrost tests attempt to characterize the heat pump operation under very humid conditions, while the low frost, steady-state data provides the systems maximum performance. The two tests will bracket the annual performance of the equipment. It should be noted that the heat pump could experience even more extreme weather conditions that cannot be easily characterized in the laboratory nor with an EnergyPlus simulation. When the heat pump operates in snow or near freezing rain, the rates of ice accumulation, performance degradation, and defrost cycle frequency are expected to increase dramatically.

The data revealed that a piecewise regression is needed, because a cusp at 25°F was observed (Figure 18). This discontinuity is due to the heat pump control logic, which ends the defrost cycle at different outdoor coil temperatures above and below an outdoor air temperature of 25°F. The system has the largest capacity degradation at conditions near freezing where the air contains more moisture and is nearest the frost point. There are two distinct curves for the minimum and maximum heat pump speed. However, at outdoor conditions below 25°F, the capacity derating appears to be independent of the compressor speed. The system initiates shorter duration defrost cycles between typically 90- and 120-minute heating cycle intervals. Because the colder air contains less water vapor, frost accumulation occurs at slower rates despite the highest heat pump speeds and the coldest coil temperatures. Upon developing this regression, more tests points would help to better understand the trends at low temperatures. A few estimates were included to better approximate a regression below 25°F.

During the eleven tests performed, a total of 56 defrost cycles occurred. The COP derating was plotted using higher-fidelity averages on a cycle-by-cycle basis, as shown in Figure 19. The correlation of the COP degradation is directly proportional to the capacity degradation. This is expected because the COP is a ratio of the capacity to the heat pump input energy.

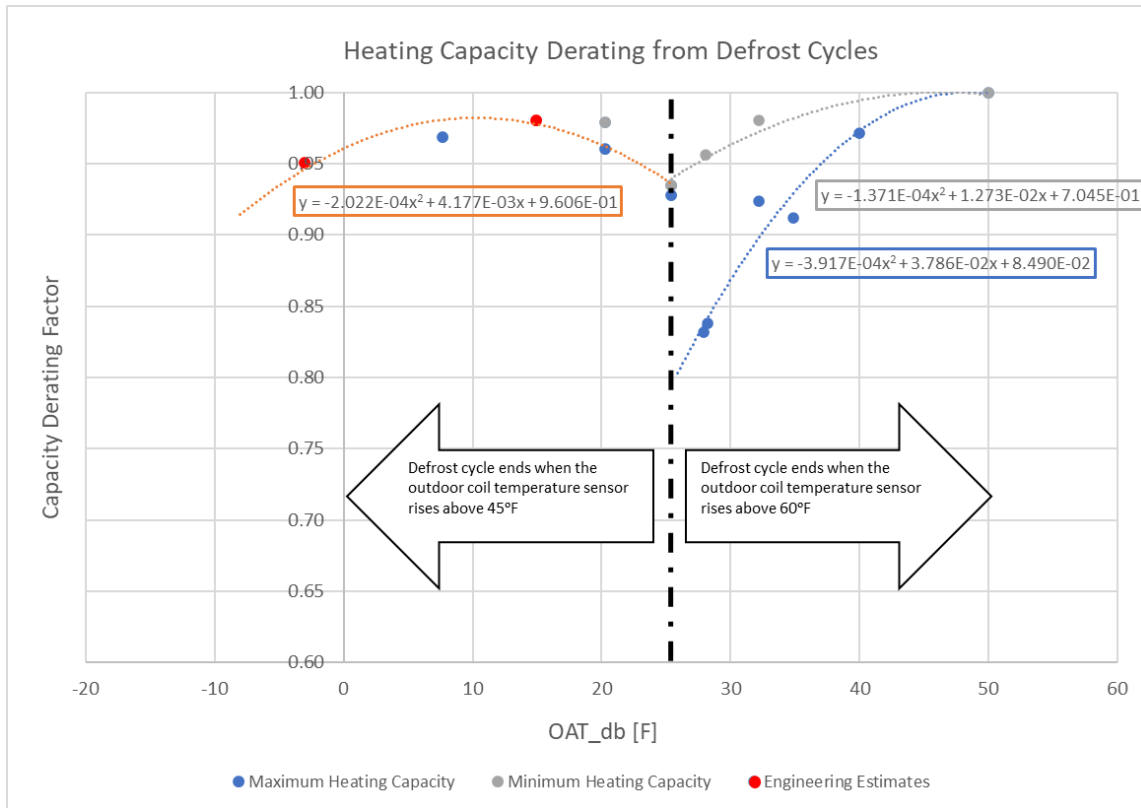


Figure 18. Estimated capacity derating factors regressions to account for defrost cycles

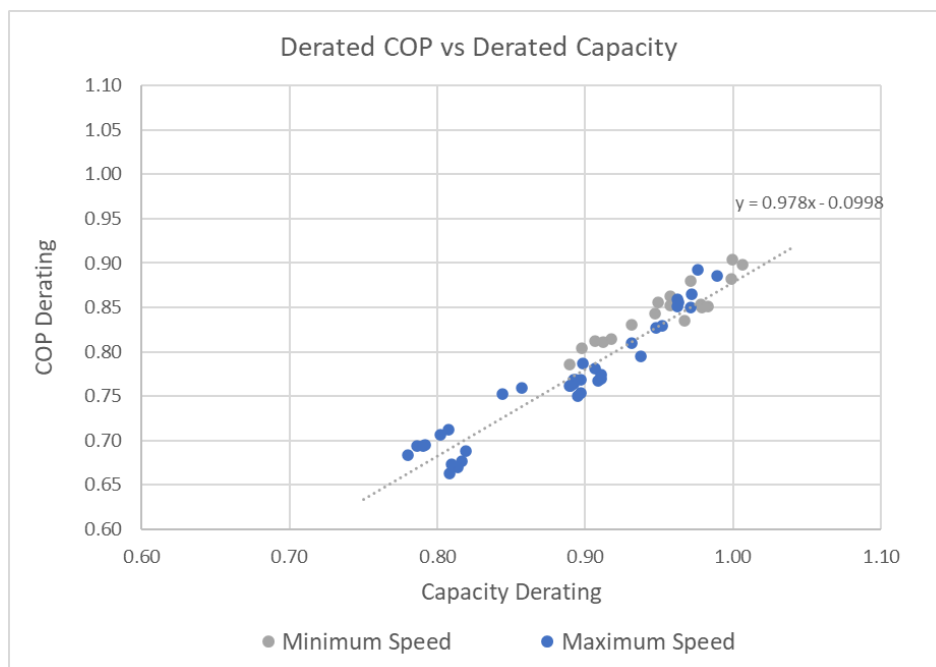


Figure 19. COP derating as a function of the capacity derating factor

4 Energy Modeling Setup

EnergyPlus 9.5 is the software used for the simulation of the advanced heat pump model. EnergyPlus is a free, open-source, cross-platform, whole-building hourly energy simulation program that engineers, architects, and researchers use to model both energy consumption—for heating, cooling, ventilation, lighting and plug and process loads—and water use in buildings. The console-based program reads input and writes output to text files.

The heat pump’s performance is simulated for three DOE prototype buildings: a single-family home, a strip mall, and a low-rise office building. These prototype building models are available on the DOE database of typical building models (referenced below). The buildings follow IECC 2021 recommendations for ASHRAE climate zone 5A. A brief description of the features of these buildings is given in Table 11. The HVAC operation, occupancy, equipment, lighting, and ventilation schedules are also defined by default in these buildings and are obtained from the ASHRAE users’ manual 2014. The buildings are simulated for the city of Chicago, using the TMY3 weather file for the Chicago O’Hare international airport.

Table 11. Summary of Different DOE Prototype Buildings Simulated

| Parameters | Single-Family Home | Strip Mall | Low-Rise Office |
|----------------------------------|--|---|---|
| Total building area (sf) | 3,565 | 22,500 | 5,502 |
| Window-wall ratio (%) | 14% | 11% | 21% |
| Hours of operation | 24/7 | Store type 1: 9:00-24:00 Store type 2: 9:00-21:00 Store type 3: 9:00-19:00 | Weekdays: 8:00-17:00 |
| Baseline HVAC system description | Single-stage heat pump with direct expansion (DX) cooling, reverse DX electric heating, and supplemental electric heat | Single-stage heat pump RTU with DX cooling, reverse DX electric heating, and supplemental electric heat | Single-stage heat pump RTU with DX cooling, reverse DX electric heating, and supplemental electric heat |
| Heating efficiency | 7.9 HSPF | 7.5 HSPF | 7.5 HSPF |
| Cooling efficiency | 13.0 SEER | 12.0 SEER | 12.0 SEER |
| Supply fan efficiency | 0.4 W/cfm | 0.5 W/cfm | 0.5 W/cfm |

For simulating the ComEd advanced heat pump, the experimental data described in the previous sections **for efficiency mode** were translated into an EnergyPlus readable format. This was done through the following process.

- The experimental data were translated from their raw form into Table:Lookup objects. These objects map the independent variables (the outdoor air dry-bulb temperature and the entering wet-bulb temperature of the coil in this case) to the capacity of the heat pump. The lookup table object is specified to use either linear or cubic interpolation independently for each input variable. For performance points outside the defined grid

space, an extrapolation method—constant or linear—is set independently for each dimension. The table also has two specified values above and below which extrapolation is not permitted.

- The `Table:Lookup` objects are referenced by the cooling capacity as a function of temperature (*CoolCapfT*) and heating capacity as a function of temperature (*HeatCapfT*) curves. For each set of these curves, a reference-rated cooling/heating capacity, COP, and a reference-rated air flow rate are specified. There are 10 such curves specified for each heating and cooling coil, and each of these curves use a `Table:Lookup` object. Each curve is representative of a particular speed of operation of the heat pump.
- The same procedure is repeated to reference `Table:Lookup` objects to Energy Input Ratio as a function of temperature curves (*EIRfT*). The Energy Input Ratio is the inverse of COP. The independent variables for the table objects are once again the entering wet-bulb temperature and the outdoor air dry-bulb temperature. 10 such curves are specified for the heating and cooling coils.
- The curves described above are referenced by `Coil:Cooling:DX:VariableSpeed` and `Coil:Heating:DX:VariableSpeed` objects. These objects in EnergyPlus simulate different speed-rated performance of the cooling and heating coils specified. In this simulation, 10 different speeds are specified.
- The two coils are wrapped in a `AirLoopHVAC:UnitaryHeatPump:AirToAir` object to complete the setup of the advanced heat pump model. These two coils are complemented by a supplemental backup electric heating coil.

For all the DOE prototype buildings referenced above, simulations were run for both a baseline case and an advanced case. The results and savings of these simulations are discussed next.

5 Energy Modeling Results

This section discusses the energy modeling results for the baseline models described in Section 4 retrofitted with a high-efficiency heat pump.

Figure 20 shows the whole-building energy savings for a single-family home retrofitted with the high-efficiency heat pump model as compared to a baseline model with a standard efficiency heat pump unit.

The single-family home prototype shows relatively lower savings (22.1%) than the other two building models represented here (29.3% for strip mall, 28% for office). This is due to the following reasons:

- The single-family home model has relatively low supply fan savings (13.1%). This is because in the baseline model for this building type, the supply fans cycle only when heating and cooling is required, and they are turned off otherwise. In the other two commercial buildings, the fans are required by the building's Uniform Mechanical Code to be operational during business hours to meet ventilation and indoor air quality requirements in compliance with the Uniform Mechanical Code.

- The magnitude of internal loads, which need to be met by the HVAC system, are also smaller in a residential building model as compared to the other two commercial building prototypes.

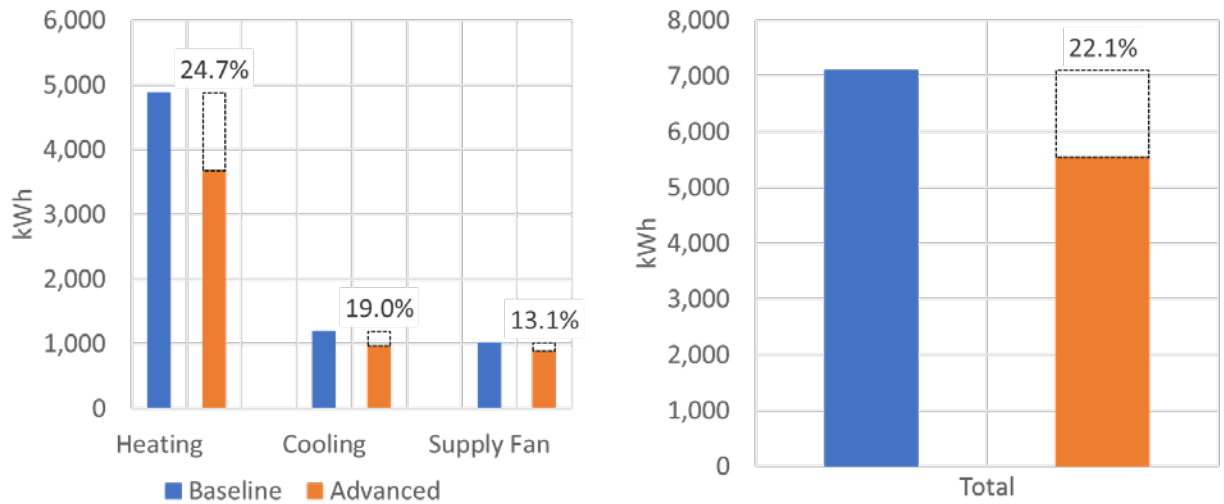


Figure 20. HVAC energy use comparison for a single-family home with the high-efficiency heat pump model. The figure on the left shows the end-use savings breakdown, and the figure on the right shows the total site energy use for the baseline and high-efficiency heat pump models.

Figure 21 shows the savings for the strip mall building prototype with a high-efficiency heat pump.

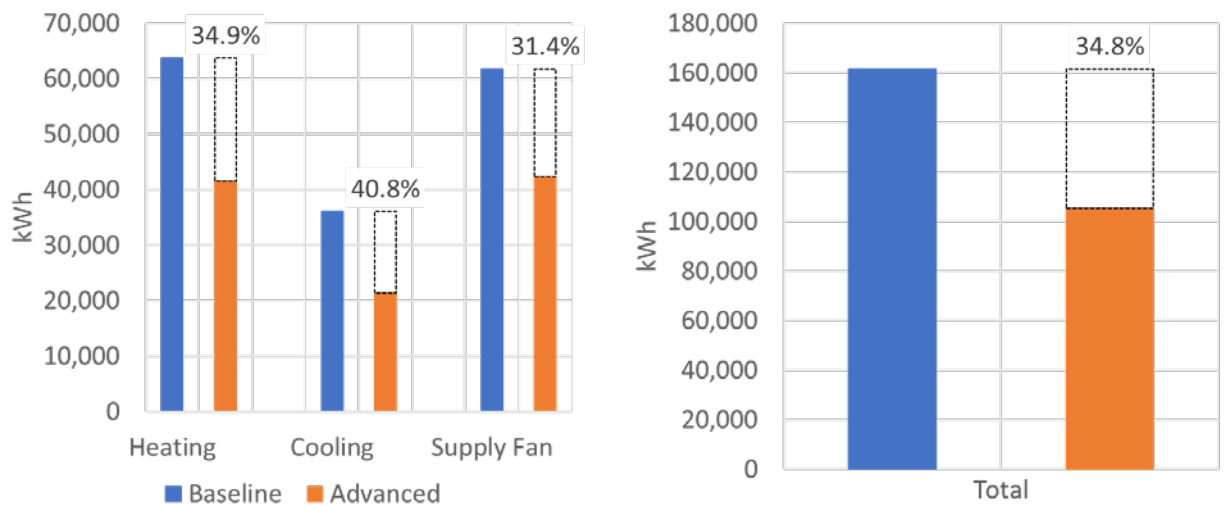


Figure 21. HVAC energy use comparison for a strip mall with the high-efficiency heat pump model. The figure on the left shows the end-use energy consumption breakdown, and the figure on the right shows the total site energy use for the baseline and high-efficiency heat pump models.

The strip mall prototype model shows the highest energy savings over its respective baseline, both in terms of percentage and in terms of absolute energy savings numbers. There are a couple of reasons for this:

- The increased absolute energy savings are likely due to the large square footage of the strip mall (see Section 4). More conditioned area means more loads to be met, and therefore higher energy usage (and subsequently higher absolute savings) for the building.
- A strip mall also has significantly higher ventilation requirements to accommodate considerably more occupied hours and loads that need to be satisfied by the HVAC system. This translates to increased time of operation and capacity of the baseline system as well as the advanced heat pump model.
- The load for the strip mall occurs coincidentally with lower ambient temperatures (due to longer operating hours). This would utilize the baseline’s strip heating coil more, leading to higher baseline energy usage. The performance of the advanced heat pump, however, would help minimize the utilization of the strip heater in the unit, and therefore realize more savings.
- The more the systems run, the more the opportunity for the advanced heat pump system to perform better and thereby reduce consumption of energy. These factors translate to more savings.

Figure 22 shows the savings for the low-rise office building prototype with a high-efficiency heat pump.

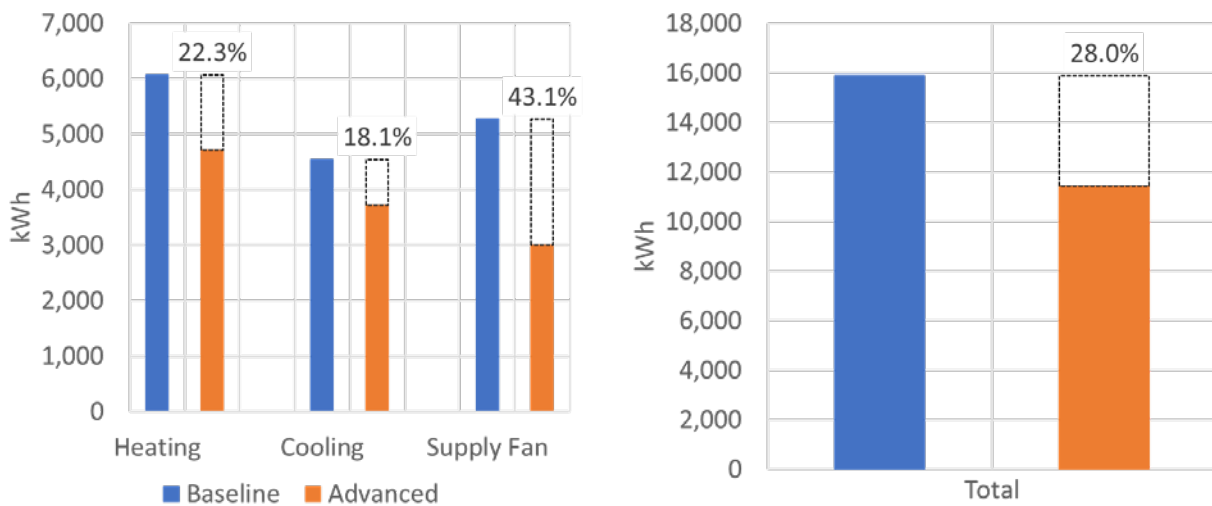


Figure 22. HVAC energy use comparison for low-rise office building with the high-efficiency heat pump model. The figure on the left shows the annual end-use energy consumption breakdown, and the figure on the right shows the total site annual energy use for baseline and the high-efficiency heat pump model.

The low-rise office building’s energy savings are comparable to the strip mall prototype. The lower ventilation requirements of the low-rise office buildings and reduced hours of operation are probably why the overall savings are slightly lower than the strip mall prototype.

6 Conclusion

Table 12 shows a summary of the energy savings for the three different prototypes simulations.

Table 12. Energy Savings Summary for the Different DOE Prototype Buildings Simulated

| Parameters | Single-Family Home | Strip Mall | Low-Rise Office |
|---|---------------------------|-------------------|------------------------|
| Heating energy savings | 24.7% | 34.9% | 22.3% |
| Cooling energy savings | 19.0% | 40.8% | 18.1% |
| Supply fan energy savings | 13.1% | 31.4% | 43.1% |
| Total (heating, cooling, and supply fan) energy savings | 22.1% | 34.8% | 28.0% |

The higher COP of the high-efficiency heat pump under Chicago’s low winter temperatures resulted in significant heating energy savings in all three buildings. The higher compressor COP also contributed to moderate annual cooling energy savings. The high-efficiency supply fan motor and variable-speed controls of the high-efficiency heat pump provided additional fan energy savings for all three building models.

The strip mall building shows the highest whole-building energy savings (29.3%) over its respective baseline. The low-rise office building’s savings are similar (28%), while the single-family home building has a slightly reduced energy savings due to reduced supply fan energy savings. Overall, all buildings show significant energy savings over their respective baseline and make a strong case for the utilization of these heat pumps.

References

AHRI. 2023. *Performance Rating of Unitary Air-Conditioning and Air-Source Heat Pump Equipment*. AHRI Standard 210/240-2023. Arlington, VA: Air-Conditioning, Heating, and Refrigeration Institute.

ASHRAE. 2019. *Standard Methods of Testing for Rating Electrically Driven Unitary Air-Conditioning and Heat-Pump Equipment*. ASHRAE Standard 37-2009. Atlanta, GA: American Society of Heating, Refrigerating and Air-Conditioning Engineers.

Carrier Corporation. 2018. Infinity Series Heat Pumps [Brochure]. <https://airmaxx.com/wp-content/uploads/2021/10/25VNA0-25VNA8-25HNB6-BROCHURE.pdf>

DOE. 2021. *EnergyPlus Energy Simulation Software*, Version 9.5. <https://energyplus.net/>. Washington, D.C.: U.S. Department of Energy.

JMP, Version 13. <https://www.jmp.com/>. SAS Institute Inc., Cary, NC, 1989-2019.

ANSI/ASHRAE. 2013. *Standard Methods for Temperature Measurement*. ASHRAE Standard 41.1-2013. Atlanta, GA: American Society of Heating, Refrigerating and Air-Conditioning Engineers.

ANSI/ASHRAE. 2014. *Standard Methods for Humidity Measurement*. ASHRAE Standard 41.6-2014. Atlanta, GA: American Society of Heating, Refrigerating and Air-Conditioning Engineers.

ANSI/ASHRAE. 2018. *Standard Methods for Air Velocity and Airflow Measurement*. ASHRAE Standard 41.2-2018. Atlanta, GA: American Society of Heating, Refrigerating and Air-Conditioning Engineers.

Wheeler, G., and Pate, M. 2016. “An alternative method for measuring air-handling unit static pressure following ASHRAE Standard 37: Scenario 1—horizontal ducts with elbows (RP-1581).” *Science and Technology for the Built Environment*, 22:4, 385-397, DOI: 10.1080/23744731.2016.1156998

Wheeler, G., Kozubal, E., and Judkoff, R. 2018. “Experimental Design and Laboratory Characterization of a Medium- and High-Efficiency Rooftop Unit for Use in Building Energy Simulations.” Presented at the 17th International Refrigeration and Air Conditioning Conference. <https://www.osti.gov/biblio/1558884-experimental-design-laboratory-characterization-medium-high-efficiency-rooftop-unit-use-building-energy-simulations>.

Appendix A. Instrumentation Plan

Table 13. Critical Experimental Measurements and Sensors

| System | Physical Location | Instrument Type |
|------------------|---------------------------------------|----------------------------------|
| Outdoor unit | Dry-bulb average inlet louver side 1 | 4 TC probes |
| Outdoor unit | Dry-bulb average inlet louver side 2 | 4 TC probes |
| Outdoor unit | Dry-bulb average inlet louver side 3 | 4 TC probes |
| Outdoor unit | Dry-bulb average inlet louver side 4 | 4 TC probes |
| Outdoor unit | Dry-bulb average outlet | 9 TC probes |
| Outdoor unit | Dew-point inlet | Dew-point hygrometer |
| Outdoor unit | Dew-point outlet | Dew-point hygrometer |
| Outdoor unit | Total power | Power meter |
| Outdoor unit | Compressor power | Power meter |
| Outdoor unit | Fan power | Power meter |
| Outdoor unit | Air flow | Avg pitot tube array |
| Outdoor unit | Outdoor unit fan speed | Optical tachometer |
| Outdoor unit | Compressor speed | Frequency/pulse meter |
| Outdoor unit | Outdoor unit coil temperature | Surface TC |
| Outdoor unit | Compressor inlet temperature | Surface TC |
| Outdoor unit | Compressor outlet temperature | Surface TC |
| Air-handler unit | Dry-bulb average inlet | 9 TC probes |
| Air-handler unit | Dry-bulb average outlet | 9 TC probes |
| Air-handler unit | Dew-point inlet | Dew-point hygrometer |
| Air-handler unit | Dew-point outlet | Dew-point hygrometer |
| Air-handler unit | Indoor unit fan speed | Optical tachometer |
| Air-handler unit | Inlet AHU ¹ mass flow rate | Laboratory nozzles |
| Air-handler unit | Outlet AHU mass flow rate | Laboratory nozzles |
| Air-handler unit | Differential pressure—inlet/outlet | Differential pressure transducer |
| Air-handler unit | Differential pressure—inlet/ambient | Differential pressure transducer |
| Air-handler unit | Total power | Power meter |
| Refrigerant line | Suction line temperature near OU | Surface TC |
| Refrigerant line | Suction line temperature near AHU | Surface TC |
| Refrigerant line | Liquid line temperature near OU | Surface TC |
| Refrigerant line | Liquid line temperature near AHU | Surface TC |
| Refrigerant line | Suction line pressure near OU | Gauge pressure transducer |
| Refrigerant line | Suction line pressure near AHU | Gauge pressure transducer |

| System | Physical Location | Instrument Type |
|-----------------------|--|----------------------------------|
| Refrigerant line | Liquid line pressure near OU | Gauge pressure transducer |
| Refrigerant line | Liquid line pressure near AHU | Gauge pressure transducer |
| Refrigerant line | Refrigerant mass flow rate | Coriolis mass flow meter |
| Refrigerant line | Refrigerant density | Coriolis mass flow meter |
| Lab | Dry-bulb ambient | TC probes |
| Lab | Dew-point ambient | Hygrometer |
| Lab | Ambient barometric pressure | Barometric pressure transducer |
| Environmental chamber | Booster/recirculation fan speed | Variable frequency drive |
| Environmental chamber | Differential pressure—inlet/outlet plenum | Differential pressure transducer |
| Environmental chamber | Differential pressure—inlet plenum/ambient | Differential pressure transducer |
| Environmental chamber | Damper—makeup air | Rotary actuator |
| Environmental chamber | Damper—bypass air | Rotary actuator |

¹ AHU = air-handler unit

Appendix B. Test Matrix

Table 14. Cooling (Wet-Coil) Steady-State Test Conditions (Comfort Mode and Efficiency Mode)

| Test Number | JMP OAT [°F] | JMP RA_db [°F] | JMP dp_Depression [°F] | Dew-point [°F] | JMP Compressor Speed [RPM] |
|-------------|--------------------|----------------------|------------------------------|-------------------|----------------------------------|
| Test1 | 92.9 | 75.7 | 25 | 50.7 | 1,850 |
| Test2 | 120 | 82 | 25 | 57 | 3,410 |
| Test3 | 55 | 82 | 18.25 | 63.75 | 4,250 |
| Test4 | 92.6 | 68 | 25 | 43 | 1,850 |
| Test5 | 55 | 68 | 25 | 43 | 4,250 |
| Test6 | 81 | 82 | 17.5 | 64.5 | 4,250 |
| Test7 | 107 | 68 | 10 | 58 | 2,661 |
| Test8 | 120 | 68 | 17.5 | 50.5 | 3,391 |
| Test9 | 120 | 82 | 10 | 72 | 4,250 |
| Test10 | 90.75 | 68 | 10 | 58 | 4,250 |
| Test11 | 81 | 75 | 18.25 | 56.75 | 3,290 |
| Test12 | 55 | 75 | 10 | 65 | 4,250 |
| Test13 | 61.5 | 82 | 25 | 57 | 1,970 |
| Test14 | 103.75 | 82 | 17.5 | 64.5 | 2,442 |
| Test15 | 113.5 | 75.7 | 10 | 65.7 | 3,050 |
| Test16 | 74.5 | 82 | 10 | 72 | 3,290 |
| Test17 | 55 | 68 | 10 | 58 | 2,930 |
| Test18 | 55 | 76.4 | 25 | 51.4 | 2,810 |
| Test19 | 113.5 | 75 | 18.25 | 56.75 | 3,050 |
| Test20 | 94 | 73.6 | 17.5 | 56.1 | 4,250 |
| Test21 | 94 | 73.6 | 10 | 63.6 | 1,970 |
| Test22 | 64.75 | 82 | 10 | 72 | 1,886 |
| Test23 | 92.7 | 82 | 17.5 | 64.5 | 1,850 |
| Test24 | 81 | 68 | 25 | 43 | 3,170 |
| Test25 | 87.5 | 82 | 25 | 57 | 4,250 |
| Test27 | 61.5 | 68 | 16.75 | 51.25 | 1,921 |
| Test28 | 61.5 | 73.6 | 16.75 | 56.85 | 1,970 |
| Test29 | 120 | 70.8 | 25 | 45.8 | 4,250 |
| Test30 | 95 | 82 | 22.75 | 59.25 | 1,970 |

Table 15. Cooling (Dry-Coil) Steady-State Test Conditions (Comfort Mode and Efficiency Mode)

| Test Number | JMP OAT [°F] | JMP RA_db [°F] | JMP dp_Depression [°F] | Dew-point [°F] | JMP Compressor Speed [RPM] |
|-------------|--------------------|----------------------|------------------------------|-------------------|----------------------------------|
| Test1 | 120 | 75 | 50 | 25 | 4,250 |
| Test2 | 94 | 82 | 50 | 32 | 4,250 |
| Test3 | 90.75 | 68 | 50 | 18 | 4,250 |
| Test4 | 55 | 82 | 50 | 32 | 4,250 |
| Test5 | 55 | 68 | 50 | 18 | 4,250 |
| Test6 | 120 | 68 | 50 | 18 | 3,410 |
| Test7 | 81 | 74.3 | 50 | 24.3 | 3,290 |
| Test8 | 77.75 | 74.3 | 50 | 24.3 | 3,290 |
| Test9 | 116.75 | 82 | 50 | 32 | 3,170 |
| Test10 | 81 | 82 | 50 | 32 | 3,170 |
| Test11 | 55 | 75 | 50 | 25 | 3,050 |
| Test12 | 100.5 | 68 | 50 | 18 | 2,330 |
| Test13 | 94 | 76.4 | 50 | 26.4 | 1,970 |
| Test14 | 61.5 | 68 | 50 | 18 | 1,970 |
| Test15 | 61.5 | 82 | 50 | 32 | 1,970 |

Table 16. Heating Steady-State Test Conditions (Comfort Mode and Efficiency Mode)

| Test Number | JMP OAT [°F] | JMP RA_db [°F] | JMP Compressor Speed [RPM] |
|-----------------------|-----------------------------|-------------------------------|---|
| Test1 | 60 | 73.6 | 3,395 |
| Test2 | 60 | 65.6 | 3,395 |
| Test3 | 49.5 | 60 | 1,850 |
| Test4 ¹ | 42.5 | 60 | 4,425 |
| Test5 ¹ | 39 | 65.6 | 4,940 |
| Test6 | 37.6 | 76 | 2,365 |
| Test7 ¹ | 35.9 | 76 | 5,198 |
| Test8 | 28.5 | 68 | 2,880 |
| Test9 | 21.5 | 60 | 4,168 |
| Test10 ¹ | 20.2 | 76 | 7,000 |
| Test11 ¹ | 19.8 | 68 | 7,000 |
| Test12 | 18 | 60 | 7,000 |
| Test13 | 18 | 67.2 | 3,138 |
| Test14 | 5 | 67.2 | 3,050 |
| Test15 | 5 | 76 | 3,050 |
| Test16 | 0.5 | 68.8 | 5,713 |
| Test17 ¹ | -0.1 | 68 | 5,970 |
| Test18 ¹ | -0.5 | 76 | 5,455 |
| Test19 ¹ | -3 | 60 | 5,455 |
| Test20 ¹ | -7 | 61.6 | 4,900 |
| Test21 ^{1,2} | 47 | 70 | 4,165 |

¹ Test was run at the maximum compressor speed limited by the mode of operation.

² AHRI 210/240 heating rating condition, tested in efficiency mode with a 43°F outdoor wet-bulb temperature.

Appendix C. Steady-State Cooling Performance

Table 17. Test Conditions and Heat Pump Cooling Performance Adjusted for Sea Level Operation in Efficiency Mode

| Test Conditions and Performance Data (Efficiency Mode) Adjusted for Sea Level Operation | | | | | | | | | | |
|---|------------------------------------|------------------------------------|------------------------|---------------------------|-----------------------------|------------------------------------|---------------------------|---------------------------------------|---------------------------|-----------|
| Test Conditions | | | | Analyzed Performance | | | | | | |
| Indoor Unit Coil Conditions | | Outdoor Unit Coil Conditions | Compressor Speed (RPM) | Dry or Wet Coil Condition | Supply Fan Flow Rate (SCFM) | External Static Pressure (in w.c.) | Supply Fan Power Draw (W) | Gross Total Cooling Capacity (kBtu/h) | Gross Sensible Heat Ratio | Gross COP |
| Entering Dry-Bulb Temperature (°F) | Entering Wet-Bulb Temperature (°F) | Entering Dry-Bulb Temperature (°F) | | | | | | | | |
| 82.0 | 67.1 | 95.0 | 1983 | Wet | 936 | -0.180 | 138 | 30.11 | 0.840 | 4.518 |
| 68.0 | 54.3 | 55.0 | 4247 | Wet | 1,392 | -0.440 | 410 | 52.27 | 0.850 | 4.918 |
| 75.0 | 68.2 | 55.0 | 4247 | Wet | 1,376 | -0.470 | 438 | 68.73 | 0.500 | 5.958 |
| 82.0 | 69.5 | 55.0 | 4247 | Wet | 1,374 | -0.470 | 437 | 70.09 | 0.610 | 6.052 |
| 76.4 | 61.2 | 55.0 | 2851 | Wet | 1,154 | -0.320 | 250 | 43.90 | 0.830 | 6.871 |
| 68.0 | 61.6 | 55.0 | 2953 | Wet | 1,156 | -0.320 | 254 | 45.78 | 0.570 | 6.839 |
| 68.0 | 58.1 | 61.5 | 1900 | Wet | 997 | -0.240 | 170 | 27.86 | 0.800 | 6.340 |
| 73.6 | 63.0 | 61.5 | 1992 | Wet | 1,051 | -0.270 | 201 | 32.67 | 0.750 | 6.921 |
| 82.0 | 65.9 | 61.5 | 1979 | Wet | 1,042 | -0.270 | 198 | 34.56 | 0.880 | 7.384 |
| 82.0 | 74.8 | 64.8 | 1871 | Wet | 941 | -0.230 | 162 | 38.96 | 0.480 | 8.875 |
| 68.0 | 54.3 | 81.0 | 3149 | Wet | 1,427 | -0.480 | 442 | 39.06 | 0.960 | 3.879 |
| 75.1 | 63.6 | 81.0 | 3270 | Wet | 1,367 | -0.460 | 421 | 47.92 | 0.730 | 4.565 |
| 82.0 | 70.0 | 81.0 | 4247 | Wet | 1,319 | -0.440 | 390 | 65.01 | 0.600 | 4.729 |
| 82.0 | 65.9 | 87.5 | 4247 | Wet | 1,323 | -0.430 | 380 | 58.04 | 0.760 | 4.029 |
| 82.0 | 74.8 | 74.5 | 3254 | Wet | 1,304 | -0.440 | 399 | 60.88 | 0.470 | 6.099 |
| 68.0 | 54.3 | 92.6 | 1827 | Dry | 889 | -0.190 | 123 | 20.10 | 1.000 | 3.456 |
| 75.7 | 60.6 | 92.9 | 1845 | Wet | 891 | -0.190 | 128 | 24.05 | 0.960 | 4.033 |
| 82.0 | 70.1 | 92.7 | 1837 | Wet | 881 | -0.200 | 133 | 30.21 | 0.700 | 5.052 |
| 68.0 | 61.7 | 90.7 | 4248 | Wet | 1,370 | -0.460 | 421 | 52.65 | 0.580 | 3.519 |
| 73.6 | 62.6 | 94.0 | 4248 | Wet | 1,356 | -0.460 | 411 | 52.63 | 0.700 | 3.403 |
| 70.8 | 56.6 | 120.0 | 4248 | Wet | 1,273 | -0.390 | 330 | 39.30 | 0.920 | 2.005 |
| 82.0 | 74.8 | 120.0 | 4248 | Wet | 1,244 | -0.420 | 356 | 58.02 | 0.470 | 2.883 |
| 73.6 | 66.9 | 94.0 | 1922 | Wet | 921 | -0.220 | 146 | 29.48 | 0.570 | 4.604 |
| 82.0 | 65.9 | 120.0 | 3402 | Wet | 960 | -0.220 | 159 | 38.96 | 0.790 | 2.603 |
| 68.0 | 57.7 | 120.0 | 3388 | Wet | 901 | -0.190 | 129 | 31.04 | 0.750 | 2.118 |
| 75.0 | 63.4 | 113.5 | 3071 | Wet | 872 | -0.180 | 122 | 35.07 | 0.700 | 2.840 |
| 68.0 | 61.7 | 107.0 | 2691 | Wet | 1,178 | -0.350 | 277 | 33.28 | 0.620 | 3.096 |
| 82.0 | 70.0 | 103.8 | 2506 | Wet | 1,125 | -0.330 | 256 | 37.41 | 0.710 | 3.871 |
| 75.7 | 69.0 | 113.5 | 3079 | Wet | 1,246 | -0.410 | 342 | 41.48 | 0.550 | 3.067 |
| 75.0 | 50.4 | 120.0 | 4248 | Dry | 1,287 | -0.390 | 325 | 40.11 | 1.000 | 2.054 |
| 82.0 | 53.4 | 94.0 | 4248 | Dry | 1,346 | -0.430 | 372 | 50.10 | 1.000 | 3.298 |
| 68.0 | 47.2 | 90.7 | 4247 | Dry | 1,350 | -0.410 | 359 | 42.87 | 1.000 | 2.975 |
| 68.0 | 46.1 | 120.0 | 3406 | Dry | 1,320 | -0.420 | 351 | 31.29 | 0.990 | 1.970 |
| 82.0 | 52.8 | 116.7 | 3272 | Dry | 1,305 | -0.420 | 354 | 38.81 | 1.000 | 2.618 |
| 68.0 | 50.3 | 100.5 | 2308 | Dry | 1,071 | -0.280 | 197 | 25.05 | 1.000 | 3.040 |
| 76.4 | 54.1 | 94.0 | 1925 | Dry | 923 | -0.210 | 137 | 23.99 | 1.000 | 3.776 |
| 68.0 | 49.6 | 61.5 | 1999 | Dry | 1,056 | -0.270 | 188 | 27.50 | 1.000 | 5.922 |
| 82.0 | 54.8 | 61.5 | 1961 | Dry | 1,041 | -0.270 | 188 | 32.67 | 1.000 | 7.062 |
| 68.0 | 45.8 | 55.0 | 4246 | Dry | 1,456 | -0.480 | 443 | 49.80 | 1.000 | 4.664 |
| 82.0 | 52.2 | 55.0 | 4246 | Dry | 1,406 | -0.460 | 416 | 57.93 | 1.000 | 5.309 |
| 75.0 | 49.5 | 55.0 | 3042 | Dry | 1,407 | -0.470 | 422 | 44.38 | 1.000 | 5.837 |
| 82.0 | 52.5 | 81.0 | 3168 | Dry | 1,401 | -0.470 | 427 | 45.57 | 1.000 | 4.471 |
| 74.3 | 48.8 | 81.0 | 3313 | Dry | 1,405 | -0.470 | 419 | 42.60 | 1.000 | 4.049 |
| 74.3 | 49.8 | 77.8 | 3294 | Dry | 1,371 | -0.440 | 390 | 42.52 | 1.000 | 4.259 |

Table 18. Test Conditions and Heat Pump Cooling Performance Adjusted for Sea Level Operation in Comfort Mode

| Test Conditions and Performance Data (Comfort Mode) Adjusted for Sea Level Operation | | | | | | | | | | |
|--|------------------------------------|------------------------------------|------------------------|---------------------------|-----------------------------|-----------------------------------|---------------------------|---------------------------------------|---------------------------|-----------|
| Test Conditions | | | | Analyzed Performance | | | | | | |
| Indoor Unit Coil Conditions | | Outdoor Unit Coil Conditions | Compressor Speed (RPM) | Dry or Wet Coil Condition | Supply Fan Flow Rate (SCFM) | External Static Pressure (in w.c) | Supply Fan Power Draw (W) | Gross Total Cooling Capacity (kBtu/h) | Gross Sensible Heat Ratio | Gross COP |
| Entering Dry-Bulb Temperature (°F) | Entering Wet-Bulb Temperature (°F) | Entering Dry-Bulb Temperature (°F) | | | | | | | | |
| 82.0 | 67.1 | 95.0 | 1979 | Wet | 644 | -0.080 | 56 | 27.75 | 0.730 | 4.460 |
| 68.0 | 54.3 | 55.0 | 4247 | Wet | 1,400 | -0.450 | 411 | 52.31 | 0.850 | 4.928 |
| 75.0 | 68.2 | 55.0 | 4248 | Wet | 1,377 | -0.470 | 437 | 68.75 | 0.500 | 5.959 |
| 82.0 | 69.5 | 55.0 | 4248 | Wet | 1,376 | -0.470 | 438 | 70.01 | 0.610 | 6.040 |
| 76.4 | 61.2 | 55.0 | 2819 | Wet | 1,151 | -0.320 | 248 | 43.45 | 0.830 | 6.890 |
| 68.0 | 61.8 | 55.0 | 2941 | Wet | 1,039 | -0.250 | 189 | 44.79 | 0.560 | 6.994 |
| 68.0 | 58.1 | 61.5 | 1930 | Wet | 729 | -0.130 | 76 | 26.91 | 0.720 | 6.613 |
| 73.6 | 63.0 | 61.5 | 1972 | Wet | 738 | -0.130 | 81 | 30.32 | 0.670 | 7.269 |
| 82.0 | 65.9 | 61.5 | 1950 | Wet | 740 | -0.130 | 82 | 31.97 | 0.770 | 7.694 |
| 82.0 | 74.8 | 64.8 | 1897 | Wet | 707 | -0.130 | 78 | 37.89 | 0.450 | 9.012 |
| 68.0 | 54.3 | 81.0 | 3166 | Wet | 1,310 | -0.400 | 343 | 38.50 | 0.940 | 3.983 |
| 75.0 | 63.5 | 81.0 | 3300 | Wet | 1,160 | -0.330 | 262 | 46.71 | 0.690 | 4.724 |
| 82.0 | 70.0 | 81.0 | 4247 | Wet | 1,319 | -0.440 | 390 | 65.04 | 0.600 | 4.730 |
| 82.0 | 65.9 | 87.5 | 4247 | Wet | 1,324 | -0.430 | 382 | 58.03 | 0.770 | 4.026 |
| 82.0 | 74.8 | 74.5 | 3309 | Wet | 1,161 | -0.350 | 282 | 60.50 | 0.450 | 6.270 |
| 68.0 | 54.3 | 92.6 | 1836 | Wet | 779 | -0.140 | 88 | 19.71 | 0.970 | 3.463 |
| 75.7 | 60.6 | 92.9 | 1840 | Wet | 756 | -0.140 | 85 | 22.84 | 0.920 | 3.975 |
| 82.0 | 70.0 | 92.7 | 1845 | Wet | 654 | -0.110 | 64 | 28.72 | 0.630 | 5.043 |
| 68.0 | 61.7 | 90.8 | 4248 | Wet | 1,370 | -0.460 | 419 | 52.64 | 0.580 | 3.519 |
| 73.6 | 62.6 | 94.0 | 4248 | Wet | 1,357 | -0.460 | 413 | 52.71 | 0.700 | 3.407 |
| 70.8 | 56.6 | 120.0 | 4248 | Wet | 1,364 | -0.450 | 402 | 39.85 | 0.940 | 1.994 |
| 82.0 | 74.8 | 120.0 | 4248 | Wet | 1,285 | -0.440 | 386 | 58.49 | 0.470 | 2.882 |
| 73.6 | 66.8 | 94.0 | 1923 | Wet | 629 | -0.100 | 57 | 27.40 | 0.520 | 4.550 |
| 82.0 | 65.9 | 120.0 | 3411 | Wet | 985 | -0.240 | 171 | 39.16 | 0.800 | 2.599 |
| 68.0 | 57.6 | 120.0 | 3402 | Wet | 903 | -0.190 | 130 | 31.14 | 0.750 | 2.113 |
| 75.0 | 63.4 | 113.5 | 3070 | Wet | 871 | -0.180 | 122 | 35.12 | 0.700 | 2.844 |
| 68.0 | 61.7 | 107.0 | 2684 | Wet | 806 | -0.160 | 100 | 31.55 | 0.570 | 3.192 |
| 82.0 | 70.0 | 103.8 | 2504 | Wet | 766 | -0.150 | 93 | 35.14 | 0.620 | 3.952 |
| 75.7 | 68.9 | 113.5 | 3074 | Wet | 866 | -0.190 | 126 | 39.06 | 0.510 | 3.134 |
| 75.0 | 50.3 | 120.0 | 4248 | Dry | 1,345 | -0.420 | 370 | 40.73 | 1.000 | 2.060 |
| 82.0 | 53.4 | 94.0 | 4248 | Dry | 1,347 | -0.430 | 373 | 50.08 | 1.000 | 3.294 |
| 68.0 | 47.2 | 90.7 | 4247 | Dry | 1,354 | -0.420 | 362 | 42.91 | 1.000 | 2.975 |
| 68.0 | 47.3 | 120.0 | 3440 | Dry | 1,183 | -0.330 | 257 | 30.24 | 1.000 | 1.949 |
| 82.0 | 53.6 | 116.8 | 3269 | Dry | 1,156 | -0.330 | 250 | 37.18 | 1.000 | 2.603 |
| 67.9 | 49.6 | 100.5 | 2305 | Dry | 917 | -0.200 | 130 | 23.46 | 1.000 | 2.968 |
| 76.4 | 53.5 | 94.0 | 1941 | Dry | 812 | -0.160 | 98 | 22.89 | 1.000 | 3.702 |
| 68.0 | 48.4 | 61.5 | 1967 | Dry | 929 | -0.200 | 133 | 26.05 | 1.000 | 5.977 |
| 81.9 | 54.2 | 61.5 | 1940 | Dry | 916 | -0.200 | 133 | 30.94 | 1.000 | 7.120 |
| 68.0 | 45.7 | 55.0 | 4246 | Dry | 1,456 | -0.480 | 443 | 49.84 | 1.000 | 4.670 |
| 82.0 | 52.3 | 55.0 | 4246 | Dry | 1,406 | -0.460 | 417 | 57.90 | 1.000 | 5.309 |
| 75.0 | 49.5 | 55.0 | 3054 | Dry | 1,336 | -0.420 | 360 | 43.78 | 1.000 | 5.944 |
| 82.0 | 52.4 | 81.0 | 3160 | Dry | 1,320 | -0.420 | 358 | 44.58 | 1.000 | 4.524 |
| 74.3 | 48.9 | 81.0 | 3305 | Dry | 1,367 | -0.440 | 386 | 42.15 | 1.000 | 4.078 |
| 74.3 | 49.3 | 77.8 | 3279 | Dry | 1,366 | -0.440 | 385 | 42.31 | 1.000 | 4.264 |

Appendix D. Steady-State Heating Performance

Table 19. Test Conditions and Heat Pump Heating Performance Adjusted for Sea Level Operation in Efficiency Mode

| Test Conditions and Performance Data (Efficiency Mode) Adjusted for Sea Level Operation | | | | | | | | |
|---|------------------------------------|------------------------|---|-----------------------------------|---------------------------|---------------------------------------|-------------------------|-----------|
| Test Conditions | | | Experimental Test Result Adjusted for Sea Level Performance | | | | | |
| Indoor Unit Coil Conditions | Outdoor Unit Coil Conditions | Compressor Speed (RPM) | Supply Fan Flow Rate (SCFM) | External Static Pressure (in w.c) | Supply Fan Power Draw (W) | Gross Total Heating Capacity (kBtu/h) | T_db, Indoor_Supply (F) | Gross COP |
| Entering Dry-Bulb Temperature (°F) | Entering Dry-Bulb Temperature (°F) | | | | | | | |
| 73.6 | 60.0 | 3472 | 1,388 | -0.570 | 543 | 50.97 | 108.300 | 4.113 |
| 65.6 | 60.0 | 3474 | 1,402 | -0.570 | 543 | 52.29 | 100.700 | 4.511 |
| 60.0 | 49.5 | 1802 | 1,166 | -0.370 | 285 | 26.11 | 81.200 | 4.931 |
| 60.0 | 42.5 | 4612 | 1,389 | -0.550 | 513 | 53.53 | 96.300 | 3.735 |
| 65.6 | 39.0 | 5022 | 1,370 | -0.550 | 508 | 54.24 | 102.900 | 3.263 |
| 70.0 | 47.0 | 4165 | 1,371 | -0.550 | 517 | 51.68 | 105.600 | 3.668 |
| 76.0 | 37.6 | 2218 | 853 | -0.220 | 132 | 24.82 | 103.000 | 3.405 |
| 68.0 | 28.5 | 2701 | 819 | -0.200 | 117 | 26.92 | 98.400 | 3.244 |
| 76.0 | 35.9 | 5414 | 1,329 | -0.550 | 495 | 53.42 | 113.800 | 2.691 |
| 60.0 | 21.5 | 4187 | 1,027 | -0.310 | 213 | 36.42 | 92.900 | 2.984 |
| 76.0 | 20.2 | 6998 | 1,346 | -0.560 | 504 | 48.85 | 110.300 | 1.997 |
| 68.0 | 19.8 | 7000 | 1,361 | -0.560 | 505 | 52.68 | 104.500 | 2.187 |
| 60.0 | 18.0 | 6998 | 1,382 | -0.550 | 504 | 51.99 | 95.400 | 2.363 |
| 67.2 | 18.0 | 3035 | 849 | -0.210 | 127 | 25.54 | 95.100 | 2.860 |
| 68.8 | 0.5 | 5658 | 886 | -0.220 | 142 | 26.77 | 96.900 | 1.691 |
| 68.0 | -0.1 | 5904 | 902 | -0.230 | 149 | 28.06 | 96.900 | 1.703 |
| 76.0 | -0.1 | 5978 | 912 | -0.240 | 155 | 23.73 | 100.300 | 1.382 |
| 60.0 | -3.0 | 5462 | 856 | -0.200 | 125 | 27.58 | 89.800 | 1.931 |
| 61.6 | -6.9 | 4838 | 792 | -0.170 | 102 | 22.51 | 87.900 | 1.836 |
| 67.2 | 5.0 | 3006 | 695 | -0.140 | 75 | 19.26 | 92.800 | 2.162 |
| 76.0 | 5.0 | 3002 | 616 | -0.110 | 57 | 16.36 | 100.500 | 1.760 |

Table 20. Test Conditions and Heat Pump Heating Performance Adjusted for Sea Level Operation in Comfort Mode

| Test Conditions and Performance Data (Comfort Mode) Adjusted for Sea Level Operation | | | | | | | | |
|--|------------------------------------|------------------------|---|-----------------------------------|---------------------------|---------------------------------------|-------------------------|-----------|
| Test Conditions | | | Experimental Test Result Adjusted for Sea Level Performance | | | | | |
| Indoor Unit Coil Conditions | Outdoor Unit Coil Conditions | Compressor Speed (RPM) | Supply Fan Flow Rate (SCFM) | External Static Pressure (in w.c) | Supply Fan Power Draw (W) | Gross Total Heating Capacity (kBtu/h) | T_db, Indoor_Supply (F) | Gross COP |
| Entering Dry-Bulb Temperature (°F) | Entering Dry-Bulb Temperature (°F) | | | | | | | |
| 73.6 | 60.0 | 3472 | 1,385 | -0.570 | 541 | 50.99 | 108.400 | 4.115 |
| 65.6 | 60.0 | 3474 | 1,402 | -0.570 | 543 | 52.36 | 100.800 | 4.530 |
| 60.0 | 49.5 | 1805 | 808 | -0.180 | 108 | 26.12 | 89.900 | 5.006 |
| 60.0 | 42.5 | 4463 | 1,386 | -0.550 | 507 | 52.27 | 95.500 | 3.810 |
| 65.6 | 39.0 | 4708 | 1,357 | -0.530 | 490 | 51.66 | 101.400 | 3.380 |
| 76.0 | 37.6 | 2218 | 650 | -0.130 | 68 | 24.14 | 110.100 | 3.063 |
| 68.0 | 28.5 | 2700 | 721 | -0.150 | 85 | 26.44 | 101.800 | 3.078 |
| 76.0 | 35.9 | 4939 | 1,303 | -0.530 | 464 | 50.35 | 112.300 | 2.818 |
| 60.0 | 21.5 | 4178 | 992 | -0.290 | 195 | 36.98 | 94.600 | 3.010 |
| 76.0 | 20.2 | 6001 | 1,258 | -0.490 | 410 | 44.24 | 109.100 | 2.161 |
| 68.0 | 19.8 | 6033 | 1,269 | -0.480 | 406 | 46.19 | 102.200 | 2.337 |
| 60.0 | 18.0 | 6118 | 1,245 | -0.450 | 369 | 48.16 | 96.200 | 2.545 |
| 67.2 | 18.0 | 3018 | 807 | -0.190 | 111 | 25.21 | 96.100 | 2.764 |
| 68.8 | 0.5 | 5733 | 889 | -0.230 | 143 | 25.92 | 95.900 | 1.634 |
| 68.0 | 0.0 | 5927 | 906 | -0.230 | 151 | 28.58 | 97.300 | 1.715 |
| 76.0 | 0.0 | 5970 | 909 | -0.240 | 154 | 23.48 | 100.100 | 1.372 |
| 60.0 | -3.0 | 5462 | 856 | -0.200 | 126 | 27.89 | 90.200 | 1.952 |
| 61.6 | -7.0 | 4790 | 787 | -0.170 | 100 | 21.77 | 87.200 | 1.802 |
| 67.2 | 5.0 | 3022 | 666 | -0.130 | 67 | 19.21 | 93.800 | 2.141 |
| 76.0 | 5.1 | 3014 | 615 | -0.110 | 57 | 16.50 | 100.800 | 1.761 |

Appendix E. Accuracy of RSM Predictive Cooling Model Regressions

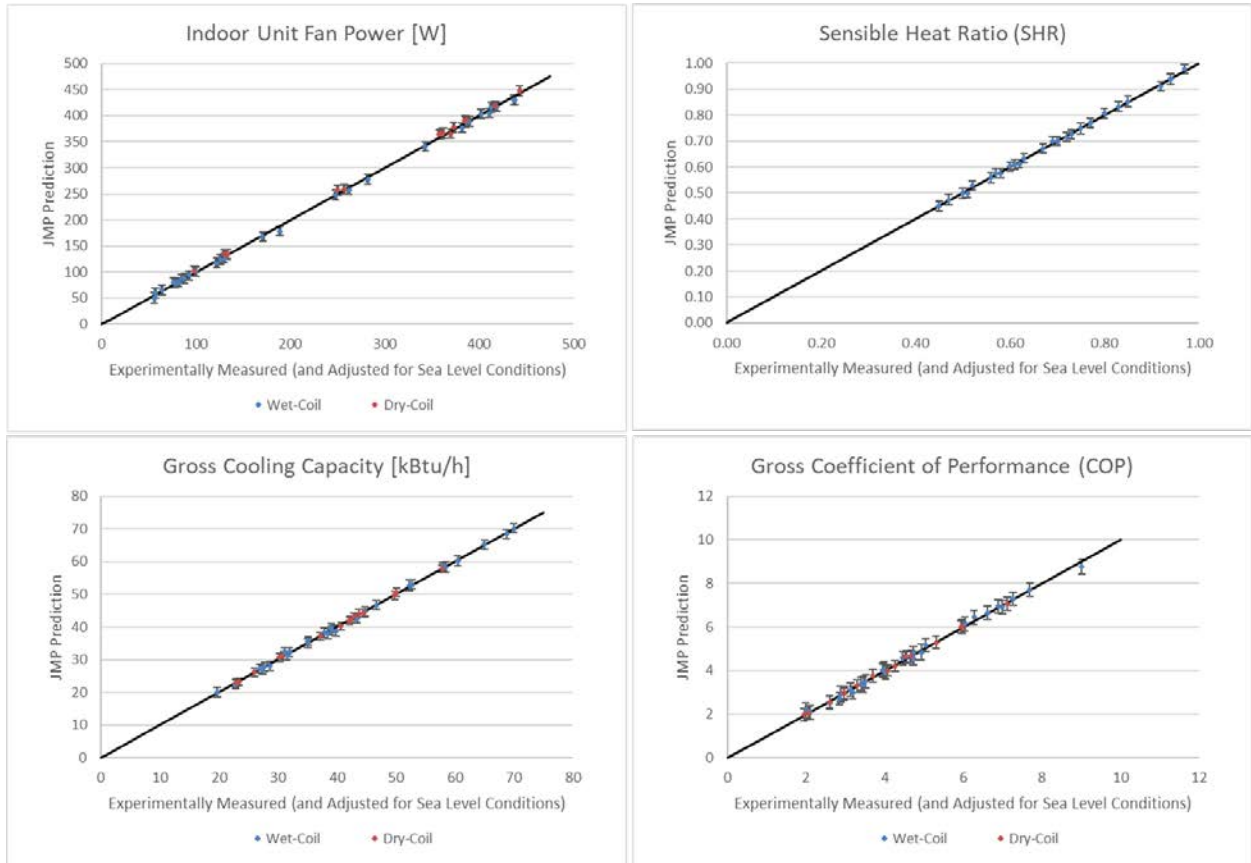


Figure 23. JMP statistical software RSM predictive model accuracy (U95) of the heat pump cooling regressions in comfort mode

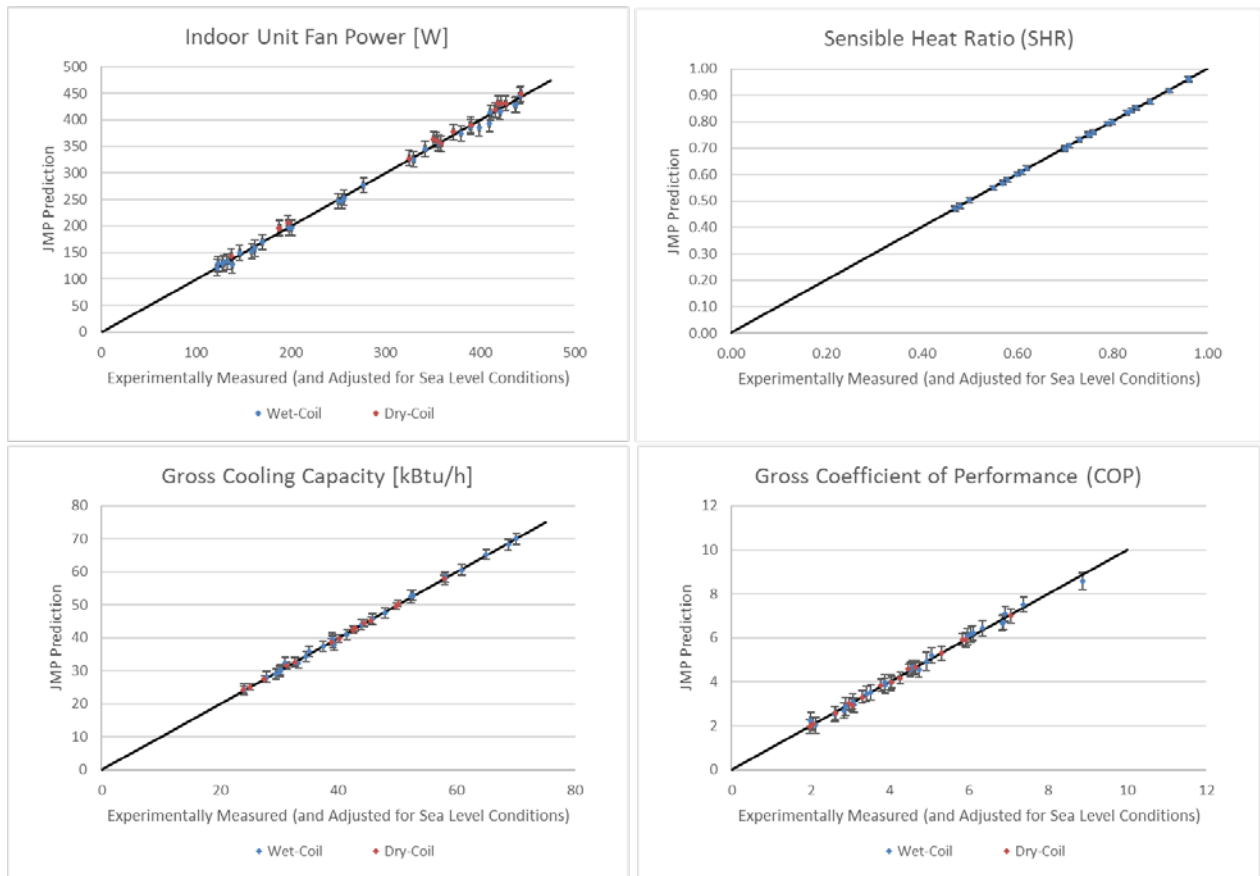


Figure 24. JMP statistical software RSM predictive model accuracy (U95) of the heat pump cooling regressions in efficiency mode

Appendix F. Accuracy of RSM Predictive Heating Model Regressions

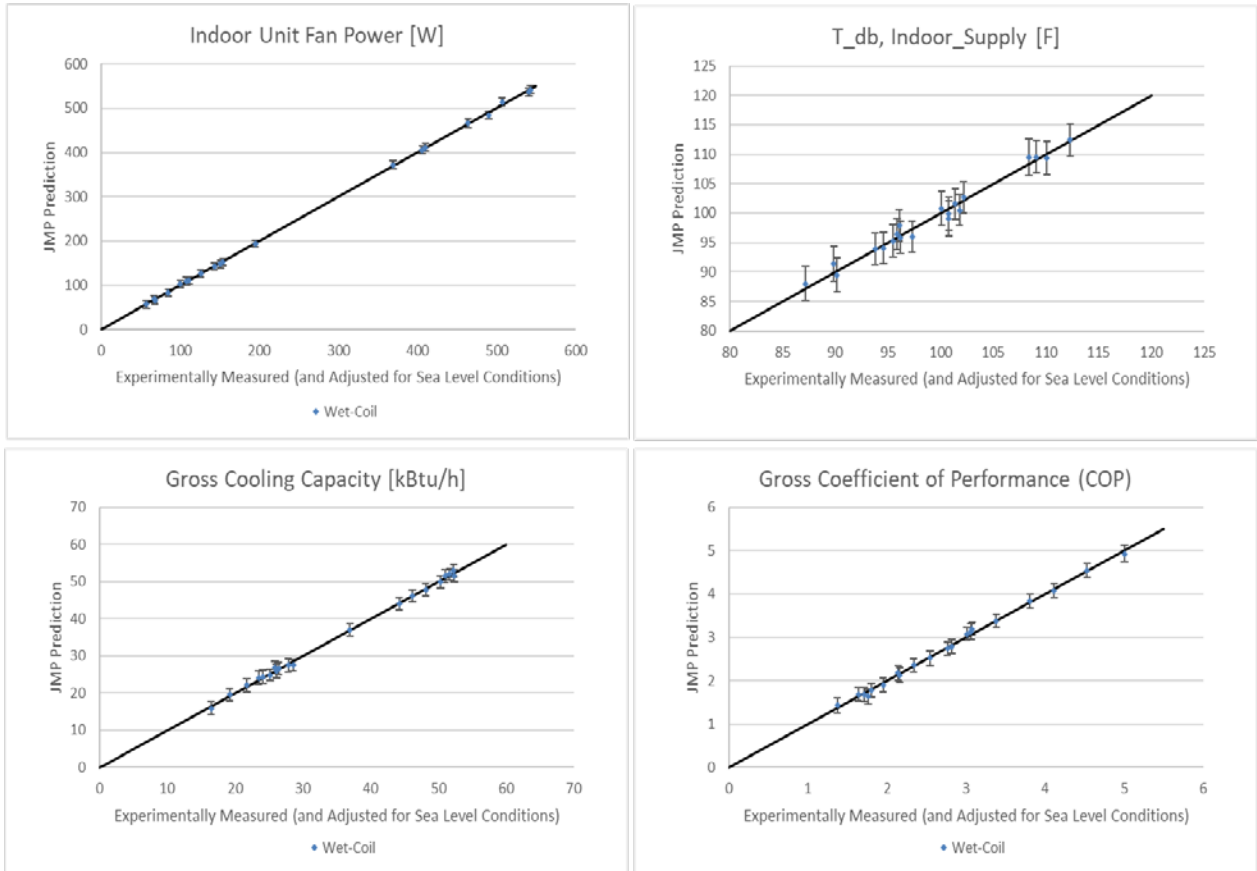


Figure 25. JMP statistical software RSM predictive model accuracy (U95) of the heat pump heating regressions in comfort mode

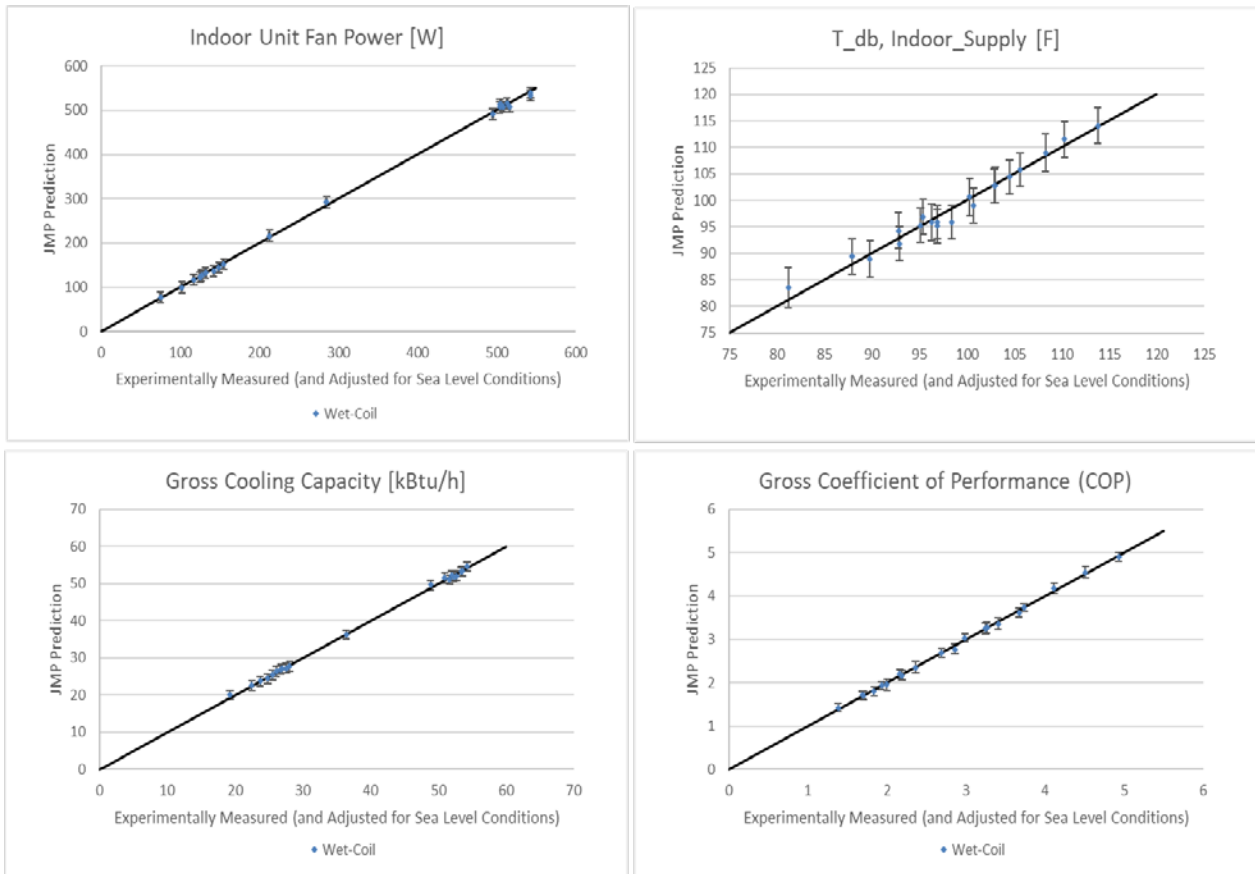


Figure 26. JMP statistical software RSM predictive model accuracy (U95) of the heat pump heating regressions in efficiency mode

Appendix G. Heating Defrost Cycle

Defrost (25VNA0)

This user interface (UI) offers 5 possible defrost interval times: 30, 60, 90, 120 minutes, or AUTO. The default is AUTO.

Defrost interval times: 30, 60, 90, and 120 minutes or AUTO are selected by the Infinity Control User Interface (dip switches are not used.)

AUTO defrost adjusts the defrost interval time based on the last defrost time as follows:

- When defrost time <3 minutes, the next defrost interval=120 minutes.
- When defrost time 3-5 minutes, the next defrost interval=90 minutes.
- When defrost time 5-7 minutes, the next defrost interval=60 minutes.
- When defrost time >7 minutes, the next defrost interval=30 minutes.

The control board accumulates compressor run time. As the accumulated run time approaches the selected defrost interval time, the control board monitors the coil temperature sensor for a defrost demand. If a defrost demand exists, a defrost cycle will be initiated at the end of the selected time interval. A defrost demand exists when the coil temperature is at or below 32°F (0°C) for 4 minutes during the interval. If the coil temperature does not reach 32°F (0°C) within the interval, the interval timer will be reset and start over.

- Upon initial power up the first defrost interval is defaulted to 30 minutes. Remaining intervals are at selected times.
- Defrost is only allowed to occur below 50°F (10°C) outdoor ambient temperature.

The defrost cycle is terminated as described below.

- When OAT is > 25°F (-3.9 °C), defrost terminates if outdoor coil temperature (OCT) > 60°F (+15.6°C) (min. 4.5 minutes)
- When OAT is <= 25°F (-3.9°C), defrost terminates if outdoor coil temperature (OCT) > 45 °F (+7.2°C) (min. 3.25 minutes)
- Or 10 minutes has passed.

At the defrost termination, the outdoor fan output (ODF) will turn on 15 seconds before the reversing valve switching.

NOTE: Compressor speed during defrost varies based on outdoor conditions.

Figure 27. Defrost embedded control logic explained in the Carrier 25VNA0 service manual